Tyrosine Phosphorylation of Membrane Proteins Mediates Cellular Invasion by Transformed Cells

Susette C. Mueller, Yunyun Yeh, and Wen-Tien Chen

Department of Anatomy and Cell Biology, Georgetown University School of Medicine, Washington, D.C. 20007

Abstract. Tyrosine phosphorylation of membrane-associated proteins is involved at two distinct sites of contact between cells and the extracellular matrix: adhesion plaques (cell adhesion and de-adhesion) and invadopodia (invasion into the extracellular matrix). Adhesion plaques from chicken embryonic fibroblasts or from cells transformed by Rous sarcoma virus contain low levels of tyrosine-phosphorylated proteins (YPPs) which were below the level of detection in 0.5-μm thin, frozen sections. In contrast, intense localization of YPPs was observed at invadopodia of transformed cells at sites of degradation and invasion into the fibronectin-coated gelatin substratum, but not in membrane extensions free of contact with the extracellular matrix. Local extracellular matrix degradation and formation of invadopodia were blocked by genistein, an inhibitor of tyrosine-specific kinases, but cells remained attached to the substratum and retained their free-membrane extensions. Invadopodia reduced or lost YPP labeling after treatment of the cells with genistein, but adhesion plaques retained YPP labeling. The plasma membrane contact fractions of normal and transformed cells have been isolated form cells grown on gelatin cross-linked substratum using a novel fractionation scheme, and analyzed by immunoblotting. Four major YPPs (150, 130, 81, and 77 kD) characterize invadopodial membranes in contact with the matrix, and are probably responsible for the intense YPP labeling associated with invadopodia extending into sites of matrix degradation. YPP150 may be an invadopodial-specific YPP since it is ~3.6-fold enriched in the invasive contact fraction relative to the cell body fraction and is not observed in normal contacts. YPP130 is enriched in transformed cell contacts but may also be present in normal contacts. The two major YPPs of normal contacts (130 and 71 kD) are much lower in abundance than the major tyrosine-phosphorylated bands associated with invadopodial membranes, and likely represent major adhesion plaque YPPs. YPP150, paxillin, and tensin appear to be enriched in the cell contact fractions containing adhesion plaques and invadopodia relative to the cell body fraction, but are also present in the soluble supernate fraction. However, vinculin, talin, and α-actinin that are localized at invadopodia, are equally concentrated in cell bodies and cell contacts as is the membrane-adhesion receptor β_1 integrin. Thus, tyrosine phosphorylation of the membrane-bound proteins may contribute to the cytoskeletal and plasma membrane events leading to the formation and function of invadopodia that contact and proteolytically degrade the extracellular matrix; we have identified several candidate YPPs that may participate in the regulation of these processes.

METASTATIC tumor cells interacting with the extracellular matrix exhibit cell-surface extensions that possess an aggressive function, namely extracellular matrix degradation, adhesion, and invasion (11, 20, 29). These cellular extensions identified in Rous sarcoma virus (RSV)[1]-transformed chicken embryo fibroblasts (CEF[RSV-CEF]) cultured on matrix substratum are called invadopodia and are responsible for the invasion of transformed cells through the extracellular matrix (10, 34). Invadopodia possess two unique activities: an extracellular matrix-degrading proteolytic activity (11); and an intracellular, phosphokinase activity, $pp60^{v\text{-}src}$ (12). The v-src gene product $pp60^{v\text{-}src}$ is a tyrosine-specific kinase located primarily at the cytoplasmic face of the plasma membrane of transformed cells (5). Transformation of embryonic chicken cells by $pp60^{v\text{-}src}$ causes an extensive reorganization of contact patterns, which led to the classic observations of reduced adhesion (44, 48) and rounded morphology (46). The reduction of the number and size of adhesion plaques is concomitant with the formation of invadopodia, "rosettes" (13) or "podosomes" (41) after

Please address all correspondence to Wen-Tien Chen, Department of Anatomy and Cell Biology, Georgetown University Medical School, 3900 Reservoir Road, N.W., Washington, D.C. 20007.

1. *Abbreviations used in this paper*: CEF, chicken embryo fibroblasts; RSV, Rous sarcoma virus; RSVCEF, chicken fibroblasts transformed by a wild-type Schmidt-Ruppin strain SRA; YPP, tyrosine-phosphorylated protein.

cellular transformation. Invadopodial membranes are more labile than other adhesion sites, such as focal and close contacts (10). Fibronectin-degrading proteases have been identified on the invadopodia of RSV-transformed cells which are believed to facilitate turnover of cell-surface fibronectin, thus, detaching cell membranes from adhesion sites (11, 15).

Tyrosine-phosphorylation of proteins in target cells mediates signal transduction (43). Tyrosine-phosphorylation is also associated with proteins involved in regulating membrane protein trafficking through the cell such as in endocytosis (18) and in acrosomal exocytosis (39). $Pp60^{c\text{-}src}$ is localized at the growth cone during neurite extension, a normal invasive process occurring during development (32). In addition, autocrine motility factor (20) and growth factors such as bFGF (38) and transforming growth factor-α (16) can cause scattering of tumor cells and induce an increase in cell motility. Some of these motility factors bind to receptors that are tyrosine kinases (7), and thus potentially could modulate invadopodia function, since the activity of invadopodia requires cell-surface motility events (10).

A number of interesting tyrosine-phosphorylated substrates have been identified in recent years which are associated with the membrane and which may play a role in cellular invasion including the integrin-adhesion receptors and cytoskeletal-adhesion plaque proteins (8, 14, 27, 42). Integrin participates in the adhesion of invadopodia during cellular invasion (34) and its phosphorylation after transformation may alter cellular adhesion (3, 21, 23, 40). It is likely that integrins and membrane-associated proteases responsible for extracellular matrix degradation are localized together in the membranes in invadopodia (34). Adhesion to fibronectin would thus concomitantly facilitate degradation of fibronectin (4, 9) and its subsequent endocytosis (34). Furthermore, ligation and aggregation of integrin at the cell surface stimulates cellular production of matrix metalloproteinases (45). Integrin phosphorylated on tyrosine residues may interact with receptors or tensin containing SH2 domains which are localized at subcellular sites of invasion (8, 14, 28). These interactions might provide the means by which the adhesive functions of integrin could be coupled to nearby extracellular matrix-degrading proteases during migration and invasion. Furthermore, localized changes in integrin phosphorylation could promote transmembrane signals such as those stimulating the secretion of matrix metalloproteinases in fibroblasts (45).

We have established an in vitro model to identify the subcellular expression of invasiveness which uses a recently developed method of growing cells on fibronectin-coated, gelatin beads (36). Using this approach, it was demonstrated that cells exhibit dynamic responses in organization of the integrin-fibronectin receptor and talin upon initial contact (10 min) with fibronectin beads (36). After 1 h in culture, invadopodia extend from the transformed cells extracellularly into sites of bead matrix-degradation which are easily visualized (34). Here, we used specific antiphosphotyrosine antibodies to detect tyrosine-phosphorylated proteins (YPPs) in cells actively invading fibronectin-coated, gelatin beads. We found that in transformed cells, high levels of YPPs were concentrated at the plasma membrane of invadopodia which degraded and subsequently invaded the fibronectin-coated, gelatin substratum. Low levels of YPPs were found in untransformed cell-adhesion sites. Both degradative and motile activities of the invadopodia were inhibited by genistein, an inhibitor of tyrosine-specific kinases (1, 2). These properties of the invadopodia, thus, distinguish them from other membrane extensions such as dorsal surface folds, ruffles, lamellipodia, or filopodia, as well as from membrane processes of the ventral surface that extend into preexisting niches of the substratum. In addition, we have designed a method for isolating the membranes that contact fibronectin-coated, gelatin substrata from both normal and transformed cells. The molecular mass profiles of YPPs from adhesion plaques of normal cells are compared with YPPs from invadopodia of transformed cells by immunoblotting contact membrane fractions with anti-YPP antibodies. Four major YPPs were identified from isolated transformed cell contacts which may participate in invadopodial function. Our results suggest that the enhanced phosphorylation of tyrosine-containing proteins by $pp60^{v\text{-}src}$ may directly contribute to the formation and function of the extracellular matrix-degrading structures, invadopodia.

Materials and Methods

Culture of Normal (CEF) and Transformed (RSVCEF) Cells on Gelatin Substratum

CEF and RSVCEF were cultured on rhodamine-conjugated fibronectin coupled to beads and fixed according to previously described methods (34, 36). Alternatively, cells were cultured on thick, hydrated gelatin films on coverslips, a modification of the method of Chen et al. (11). The gelatin films were rehydrated in 150 mM NaCl/10 mM phosphate buffer, pH 7.4, PBS at 4°C for 10 min and briefly fixed in 0.5% glutaraldehyde. For biochemical experiments, cells were cultured overnight at 41°C on unlabeled, cross-linked gelatin films in tissue culture dishes. The films were prepared by coating dishes with PBS containing 2.5% gelatin and 2.5% sucrose, melted, and cooled to 50°C. Excess solution was aspirated, the dishes cooled, and the films then fixed by 2.0% glutaraldehyde in PBS for 15 min at room temperature. Films were washed in PBS or deionized water and quenched for at least 1 h at room temperature with DME (Cellgro, Mediatech, Inc., Herndon, VA). Gelatin films were stored at 4°C with the addition of 2 mg/ml penicillin, and 20 U/ml streptomycin. Cells were seeded at subconfluent densities onto the beads (34,36) or onto films in dishes in culture medium consisting of DME, 1% chicken serum, 4% FBS, 10% tryptose phosphate broth, 200 μg/ml penicillin, and 2 U/ml streptomycin. In the case of incubation with 5 μg/ml genistein (ICN Biomedicals, Inc., Costa Mesa, CA), cells were allowed to attach to cross-linked gelatin beads or films at 41°C for the times indicated in the figure legends and then genistein was added to the culture medium.

Immunocytochemistry: Light and Electron Microscopy

Fixed cells were processed for either 0.1- or 0.5-μm thin, frozen sectioning using an Ultracut E43 ultramicrotome (Reichart Jung, Vienna) equipped with FC4D Low-Temperature Sectioning system as previously described (34). For immunofluorescent labeling of cells cultured on rhodamine–fibronectin cross-linked gelatin beads, 0.5-μm thin, frozen sections were labeled indirectly first with primary antibodies, either mouse monoclonal 1G2 directed against YPPs (Oncogene Science, Inc., Uniondale, NY) or mouse monoclonal 4G10 (Upstate Biotechnology Inc., Lake Placid, NY), and then with a fluorescein conjugate of goat antibody to mouse IgG. For demonstration of antibody specificity for phosphotyrosine residues of YPPs, sections were also labeled with monoclonal 1G2 or 4G10 in the presence of 1 mM *O*-phospho-L-tyrosine (Boehringer Mannheim Biochemicals, Indianapolis, IN).

CEF infected with wild-type or mutant ts68 RSV (12) were cultured on thick, fluorescent, fibronectin cross-linked gelatin films overnight and then extracted with 0.5% Triton X-100 following fixation (12). Fixed cells were labeled with anti-YPP antibodies as described above. Cells were also labeled with mouse mAb against paxillin (Zymed Laboratories, South San Francisco, CA) or rabbit antitensin (a kind gift from L.-B. Chen, Harvard University, Boston, MA). Primary antibodies were followed by rhodamine-

conjugated secondary antibodies in the case that fibronectin was conjugated to fluorescein.

Unlabeled, cross-linked, gelatin-coated coverslips containing sheared cell membrane fragments were labeled for invadopodia using rat monoclonal CP1 which stains invadopodia co-localizing with sites of substrate degradation (10), followed by fluorescein-conjugated goat anti-rat secondary antibody. Coverslips were also double labeled for β_1 integrin and actin using rat monoclonal ES238 (35), followed by fluorescein-conjugated goat anti-rat secondary antibody and rhodamine-conjugated phalloidin (Molecular Probes, Inc., Eugene, OR). ES238 recognizes the extracellular epitope of the β_1 subunit of avian integrin (35).

After immunolabeling, cells, contacts, or 0.5-μm thin, frozen sections were incubated for 5 min at room temperature with 5 mg/ml sodium borohydride in PBS to quench glutaraldehyde-induced autofluorescence, washed, and then mounted for microscopy (34). They were observed with a Zeiss Photomicroscope III (Carl Zeiss, Inc., Thornwood, NY) equipped with epifluorescence and a Planapo 63×/1.4 phase 3 objective. Whole cell-bead aggregates were observed by Nomarski differential, interference-contrast microscopy and a Neofluor 40×/0.8 N.A. water-immersion objective. Immunoelectron microscopy of cell-bead aggregates was performed as described previously (34). 0.1-μm thin, frozen sections were double labeled using rat monoclonal CP1 and rabbit polyclonal antiintegrin complex antibody (34), followed by 10-nm gold conjugated to goat anti-rabbit secondary antibody and 5-nm gold conjugated to goat anti-rat secondary antibody. Sections were observed and photographed using an electron microscope (1200EX, JEOL USA, Peabody, MA).

Semiquantitative analysis of YPP labeling in invadopodia and adhesion plaques was carried out on cells from a single negative using an image analysis system (IBAS 2000, Carl Zeiss) with a processor (Kontron Aiag, Kontron Analytical, Redwood City, CA). The image of cells within one negative was digitized and the ODs of the contact sites were obtained. Contact sites were classified as invadopodia or adhesion plaques and the sum of ODs for each type of contact was expressed in relative units for each cell (see Fig. 7).

Subcellular Fractionation of Cells Cultured on Fibronectin–Gelatin Cross-Linked Matrix

Cell contact, cell body, and supernate fractions were prepared from just confluent monolayers of cells cultured overnight on gelatin films (10-cm dishes). After washing the monolayer three times with ice cold 10 ml Tris-HCl, pH 7.4, 150 mM NaCl, TBS, the cells were washed with an additional 10 ml of a buffer designed to stabilize the membranes and cytoskeleton, 10 mM MOPS, pH 6.8, 100 mM KCl, 2.5 mM $MgCl_2$, 1 mM $CaCl_2$, 0.3 M sucrose, and 1 mM Na_3VO_4, 0.2 mM PMSF, and 0.02% NaN_3. Cell bodies were sheared away from the adherent cells in 5 ml of the same buffer (shearing buffer) using a 9-in. Pasteur pipette flamed to seal the end and produce an {L} shape. Shearing of cell bodies was accomplished by passing the 5-cm pipette rod over the surface of the gelatin using sweeping motions across and around the edges of the Petri dish for a total of 30 s. The films with adhering cellular fragments were examined by phase-contrast microscopy to ensure the removal of all cell bodies. The cell bodies were immediately centrifuged in a microfuge at top speed for 5 min at 4°C. The supernate fraction was obtained together with the pelleted cell body fraction. The cell body fraction was solubilized in 1 ml of the shearing buffer containing 1.3% Triton X-114 for 15 min by end-over-end agitation. 1.3% Triton X-114 was prepared from a stock solution of Triton X-114 which had been previously phase partitioned according to Bordier (6). During centrifugation of cell bodies, the material remaining attached to the gelatin substratum (cell contact fraction) was briefly washed 3 × 10 ml with the shearing buffer and the gelatin film was scraped into 1 ml of the shearing buffer containing 1.3% Triton X-114 and likewise subjected to end-over-end agitation for 15 min at 4°C. Partitioning of proteins to detergent and aqueous phases was accomplished by the methods of Bordier (6) and were as follows. The detergent extract was cleared by centrifugation at top speed in a microfuge and the supernate was incubated for 5 min at 37°C, and then centrifuged for 5 min at top speed. The aqueous phase was separated from the detergent phase by aspiration. The cross-linked gelatin matrix was not solubilized by these methods, as confirmed by similarly treating cell-free matrix. The cell bodies and contacts were centrifuged at top speed in the microfuge to remove detergent-insoluble material. The detergent extracts were compared on immunoblots using antiphosphotyrosine antibody following protein determinations and ethanol precipitation to concentrate the sample. Protein determinations were made using a modification of the method of Lowry (33).

Immunoblotting of Subcellular Fractions

Protein was concentrated for gels by precipitation in 70% ethanol at −20°C for a minimum of 1 h. Ethanol precipitates were resuspended in sample buffer (30). Samples were boiled and reduced in 2% β-mercaptoethanol except for the detection of integrin β_1, in which case samples were simply boiled. No detectable gelatin was released into the sampling buffer when tested using gelatin films carried through a mock culture in the absence of cells. SDS-PAGE was performed and polypeptides were transferred to nitrocellulose sheets, and incubated overnight at room temperature, by sandwiching one gel between two nitrocellulose sheets. This was then sandwiched between two sets of six layers each of No. 1 filter paper (Whatman Laboratory Products, Inc., Clifton, NJ) moistened with distilled water.

The transfer of polypeptides was monitored by staining blots with Ponceau red (Sigma Chemical Co., St. Louis, MO). YPPs were labeled using mouse mAb 4G10 antiphosphotyrosine antibody. Rabbit polyclonal antivinculin and rabbit polyclonal anti-α-actinin were visualized using previously described antibodies (36). Paxillin and tensin were visualized using the antibodies described above for immunocytochemistry. Rabbit antitalin was a kind gift from K. Burridge (University of North Carolina, Chapel Hill, NC). Immunoblotting of β_1 integrin was accomplished using rat mAb ES238 (35). Immunoblots were processed using goat anti-mouse, anti-rat, or anti-rabbit secondary antibody conjugated with horseradish peroxidase (Amersham Corp., Arlington Heights, IL). The same or a duplicate nitrocellulose blot was sequentially labeled with a mouse and then a rabbit primary antibody. In between immunoblotting experiments, the nitrocellulose blots were extensively washed and treated with 0.02% sodium azide to inactivate the horseradish peroxidase moiety of previously blotted secondary antibodies. Particular antibodies were chosen for reblotting experiments based on their quality and the molecular masses of the blotted proteins to avoid overlapping reactions. Bands were visualized on film using the ECL detection system (Amersham Corp.) according to the manufacturer's instructions. Semiquantitative analysis of bands on immunoblots was carried out using an image analysis system (Carl Zeiss) with a Processor (Kontron Analytical). The image from an exposed film was digitized and the density of the bands within equal size squares was obtained. Background densities from adjacent areas were subtracted for each band. Since equal protein loadings from each fraction were run on a single gel, the relative specific activities of a given polypeptide can be compared for the fractions from both normal and transformed cells.

Results

Role of Tyrosine Phosphorylation in Invasion

In the present study, we cultured transformed cells on fibronectin–gelatin beads (34,36) and films (11) as described in the Materials and Methods. Cellular responses to contact with the beads were examined between 30 min to 3 d after culturing using Nomarski differential, interference-contrast microscopy of cell–bead aggregates (Fig. 1). Fig. 1 shows the invasion of transformed cells into the fibronectin-coated gelatin beads by means of optical sections through the middle of the beads. Invadopodia could be detected as membrane protrusions from the ventral surface of transformed cells within the matrix beads, with increasing numbers found after longer incubations (Fig. 1, 1 *h*, 1 *d*, and 2 *d*). The addition of 5 μg/ml of genistein (1,2), an inhibitor of tyrosine-specific kinases, to the media after 1 h of cell culture, inhibited the cell-surface mobility of the transformed cells as observed using video microscopy of living cells (not shown), and invadopodial extension into the bead (Fig. 1, 1 *d* + GT), suggesting a role for tyrosine phosphorylation during invadopodia formation. RSVCEF cultured on beads for 6 h with 5 μg/ml genistein after an initial period allowing for cell attachment, and then washed and cultured overnight in the absence of genistein, were able to invade the beads in a manner similar to control cells (not shown).

Previously, we showed by thin, frozen section at the light

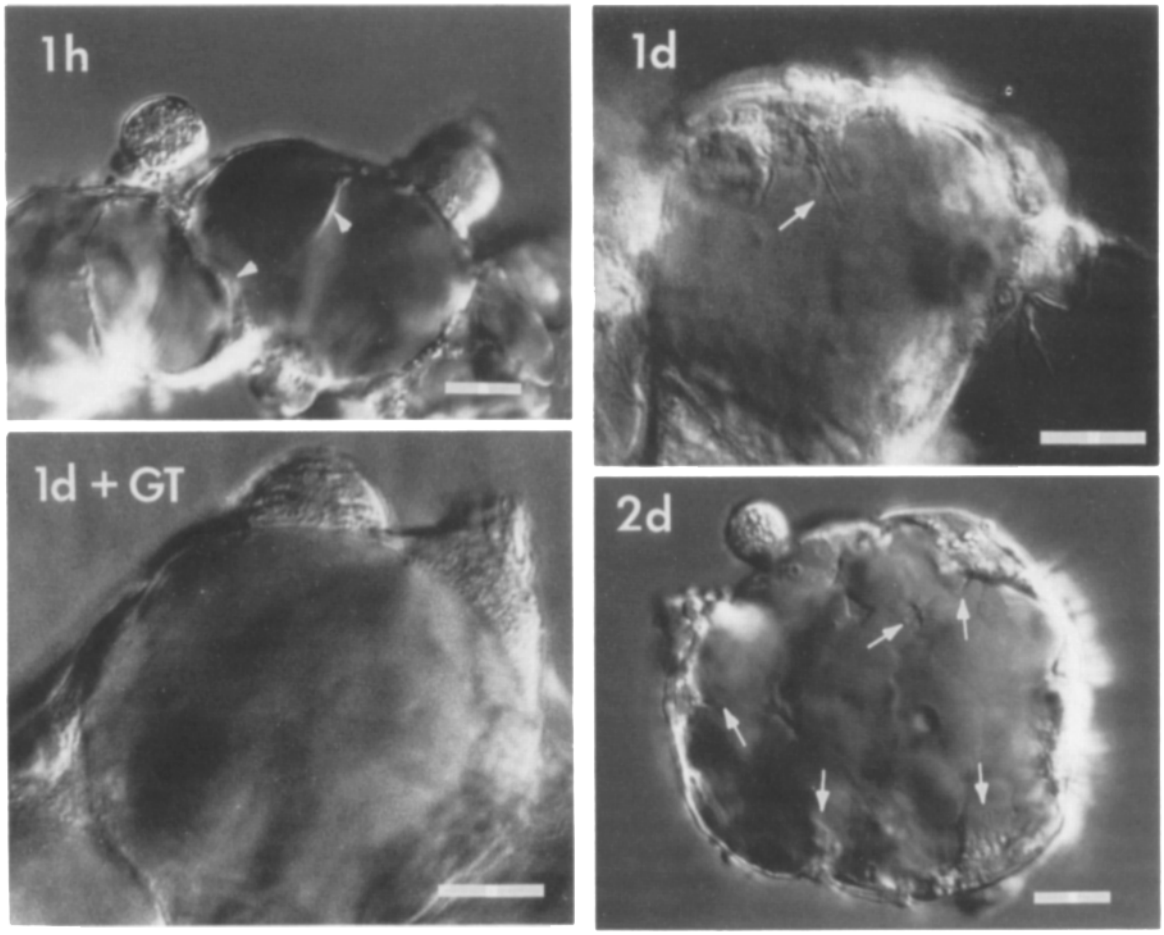

Figure 1. Invasion of transformed cells into the fibronectin-coated gelatin beads and its inhibition by genistein. Each optical section achieved using Nomarski differential interference-contrast microscopy was taken through the middle of cell–bead aggregates. (*1h*) Transformed cells cultured for 1 h with beads showing their membranes trapped in the niches of the aggregated fibronectin–gelatin beads (*arrowheads*). These structures serve as a control for the extension of cell membranes in the absence of localized matrix degradation. (*1d*) Transformed cells cultured for 1 d with beads showing the active invasion of membrane extensions of spread cells into the bead (*arrow*). (*1d + GT*) An optical section of cell–bead aggregates cultured for 1 d in the presence of 5 μg/ml genistein after a period of 1 h for cell attachment is shown. Both ruffling activity of the dorsal surface and invadopodial activity of the ventral surface of transformed cells were inhibited. The shape of the cells remained unchanged during the incubation. (*2d*) An optical section of transformed cells grown on the beads for 2 d. Numerous invadopodia have penetrated the bead (*arrows*). Bar, 20 μm.

and EM level that RSVCEF invaded fibronectin-coated, gelatin beads by extending invadopodia at sites of fibronectin–gelatin degradation and that internalized fibronectin occurred in vacuoles near invadopodia (34). Using mAbs against YPPs and low magnification views of sectioned cell–bead aggregates, we observe the striking localization of YPPs at the ventral surfaces of cells invading into fluorescent fibronectin cross-linked beads (Figs. 2–4). Degradation sites on the gelatin matrix where the rhodamine-labeled fibronectin was missing coincide with sites of invadopodia observed by phase-contrast microscopy and also with sites of YPP localization (Figs. 2 *A*, and 2 *B*, 3, 4 *A*, some examples are indicated by *arrows*). YPP labeling could be prevented in the presence of *O*-phospho-L-tyrosine (Fig. 2 *C*). Another internal control for specific YPP labeling was observed at preexisting niches in the bead where there was no YPP localization and the layer of fluorescent, fibronectin label was intact (Fig. 2 *A*, *arrowheads*). There was also no detectable YPP labeling in other sites within transformed cells including dorsal surface folds, ruffles, nucleus, and cytoplasm (Figs. 2–4). Normal CEF grown on the rhodamine–fibronectin beads did not have significant YPP labeling, or any detectable invadopodia or fibronectin degradation (Fig. 2 *D*).

Cell migration and invasion is a dynamic process, thus, sections reflect cells in various states of movement and invasion. In extensive observations of sections or whole transformed cells, we have observed that very small localized sites of fluorescent fibronectin removal are frequently coincident with YPP label. However, at large sites of fluorescent fibronectin removal or at areas where extensive degradation has taken place, YPP label is sometimes poorly coincident or the cell is nowhere to be found (also see Fig. 12 below). Therefore, bright punctate sites of labeling for YPP at the membrane may localize at active invadopodia or at putative sites of invadopodial formation which can be observed prior to obvious signs of matrix removal by the cell. These bright patches of membrane labeling are observed at early stages of invasion, 1 h after seeding onto the gelatin

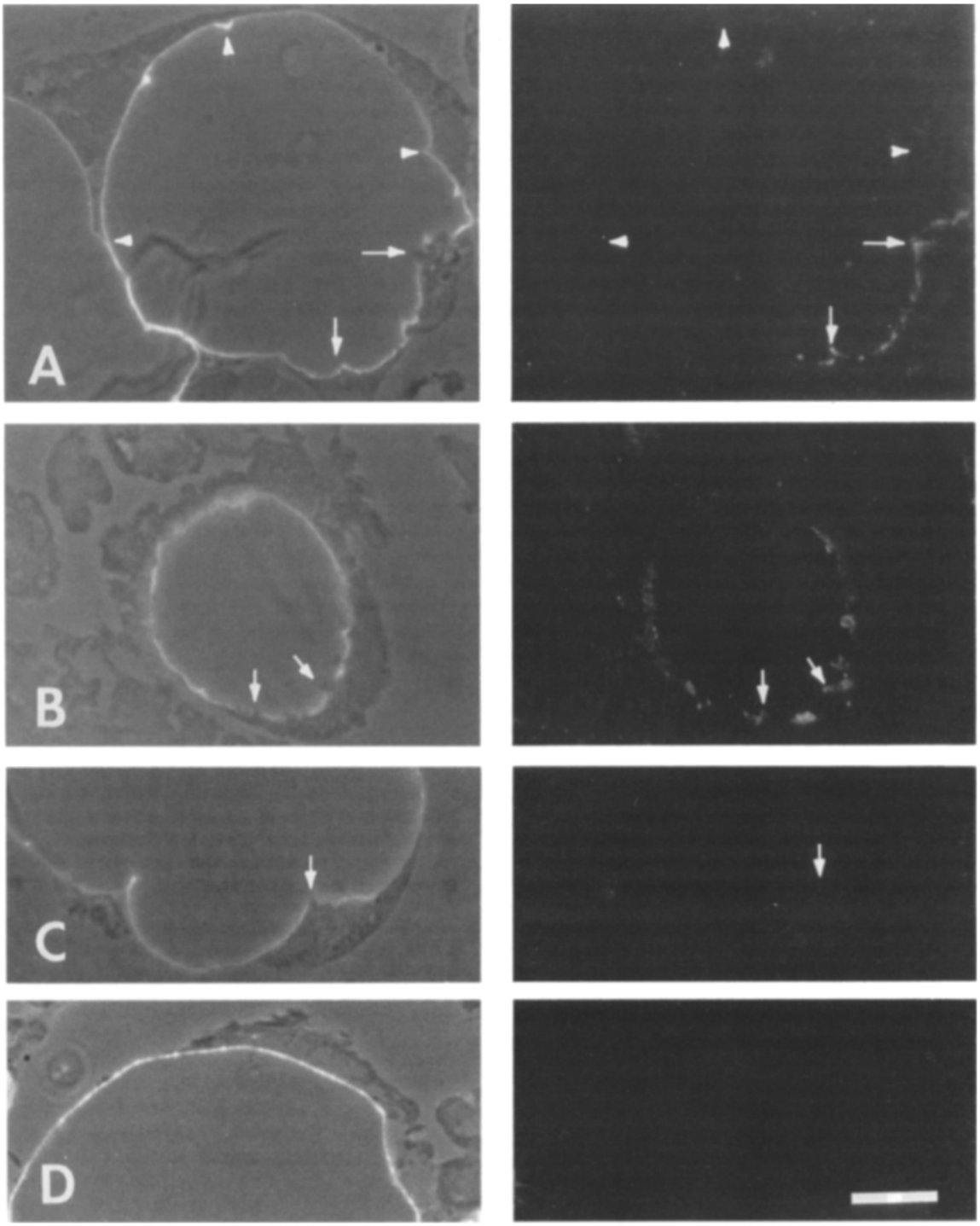

Figure 2. Specific localization of YPPs at sites of fluorescent fibronectin removal by transformed cells. For each 0.5-μm thin, frozen section of cell–bead aggregates, the left panel shows the composite phase contrast and fluorescent image of rhodamine-stained, fibronectin-coated gelatin beads; the right panel shows the immunofluorescent image of fluorescein-labeled antibody directed against YPPs. Arrows indicate examples where the invadopodia penetrated the matrix at foci, where fluorescent fibronectin coated on the bead's surface had been removed extracellularly, and where YPPs were concentrated intracellularly. (*A*) Transformed cell–bead aggregate cultured for 1 d showing invasive cells at the lower right and their invadopodia (*arrows*) as well as noninvasive cells to the left and upper right whose membranes extended into preexisting niches (*arrowheads*). Cell membranes at these niches were distinct from invadopodia and showed no YPP localization. (*B*) A section from the periphery of a cell–bead aggregate showing localization of YPPs at the invadopodia (*arrows*). Note that numerous membrane extensions on dorsal cell surfaces are free of YPP labeling. (*C*) A section of a cell–bead aggregate similar to that shown in panel *A* illustrating the specificity of YPP labeling. Immunofluorescent labeling for YPPs at the invadopodia was competitively inhibited by the addition of 1 mM of *O*-phospho-L-tyrosine during the immunolabeling procedure. (*D*) A normal CEF grown on an intact fibronectin bead shows the absence of invadopodia, fibronectin degradation, and YPP labeling. Bar, 10 μm.

substratum when matrix removal is first detectable (Fig. 3, cell at left). Most cells at this early stage, however, do not show matrix removal or the localized bright patches of YPP labeling (Fig. 3, cell at right). Invadopodia that extend into the bead far enough to be detected by phase-contrast, light microscopy typically have YPPs associated with their tips, as shown in a higher magnification view of a 0.5-μm frozen section (Fig. 4, *A* and *A'*). Immunostaining of pp60$^{v\text{-}src}$ occurs more broadly over the invadopodia, as shown in another high magnification view (Fig. 4, *B* and *B'*).

To give a measure of the correlation among matrix degradation, presence of invadopodia, the pp60$^{v\text{-}src}$ tyrosine kinase, and YPP immunolabeling, we determined the percentage of cells that were associated with matrix degradation (fluorescent fibronectin removal), and that were immunostained for pp60$^{v\text{-}src}$ (mAb EB7), invadopodia (mAb CP1), and YPP (mAb 1G2) localization in thin, frozen sections of cell–bead aggregates (Table I). The majority (81%) of RSVCEF contained detectable staining for pp60$^{v\text{-}src}$, although in ~40% of the cells, the labeling was diffuse rather than localized at the membrane. Approximately 56% of cells contained YPP label, and 38% CP1 staining. CP1 monoclonal antibody, although not adequate for immunoblotting, is an excellent morphological marker for invadopodia (10). Fibronectin degradation was observed in ~48% of RSVCEF. In ~7% of normal cells, YPP labeling could be detected in the frozen, thin sections, whereas no degradation or invadopodia was detected. Together, these results suggest a role of the pp60$^{v\text{-}src}$ tyrosine kinase in tyrosine phosphorylation of membrane-associated proteins and in the formation of invadopodia.

To obtain en face views of the YPP labeling pattern on ventral membranes of intact cells including adhesion plaques, we used YPP labeling of detergent-extracted cells that were cultured on fluorescently labeled fibronectin films. Cells infected with a temperature-sensitive mutant of pp60$^{v\text{-}src}$ (12) were used to localize YPPs in cells grown at the nonpermissive (Fig. 5 *A*) or permissive temperature for transformation (Fig. 5 *B*). The cells were cultured for 4 h at the nonpermissive temperature (41°C) on thick, cross-linked gelatin films coated with rhodamine–fibronectin and some cultures were shifted to the permissive temperature (36°C) for cell transformation overnight. Immunostaining of coverslips containing equal cell numbers was used so that levels of staining would be roughly comparable. A low level of YPP staining can be detected in adhesion sites of cells that appeared normal or transformed (Fig. 5 *A* and *B*, *arrowheads*). However, invasive cells were detected at the temperature permissive for transformation, and in these cells, more intense YPP label co-localizes with sites of fluorescent fibronectin removal in a rosette pattern (Fig. 5 *B*, *arrow*). The intense labeling for YPP at sites of degradation correlates with the YPP labeling of invadopodia detected in thin, frozen sections.

In similar experiments to those shown in Fig. 5, cells infected with the temperature-sensitive mutant for transformation (ts68) were cultured for 4 h at the nonpermissive temperature, and then cultured overnight in the presence or absence of genistein at the permissive temperature for trans-

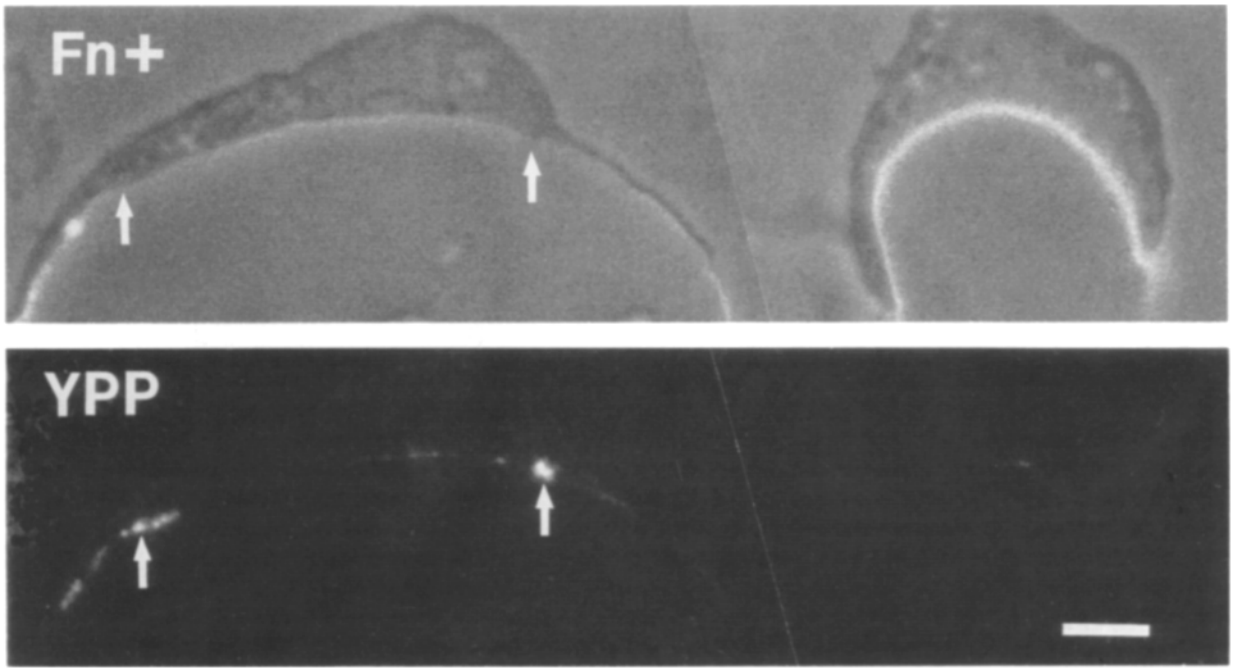

Figure 3. YPP localization and formation of invadopodia during an early stage of cell invasion. Cells were cultured on rhodamine–fibronectin beads as described in Fig. 2, except that the cells were fixed within 1 h. The same field is visualized in two ways. Top (*Fn+*) a composite of a phase-contrast image and a fluorescent image of rhodamine–fibronectin to define cell–bead boundaries and to reveal areas where fibronectin label is removed from the bead surface, and below (YPP) indirect immunofluorescence to reveal the localization of YPPs in cells. Small invadopodia had formed at 1 h (*arrows*) where cells locally degraded the labeled fibronectin surface. Membrane-associated proteins at these small invadopodia exhibited elevated levels of phosphorylation. The cell at right shows no invadopodial protrusions and YPP labeling is barely apparent. Bar, 5 μm.

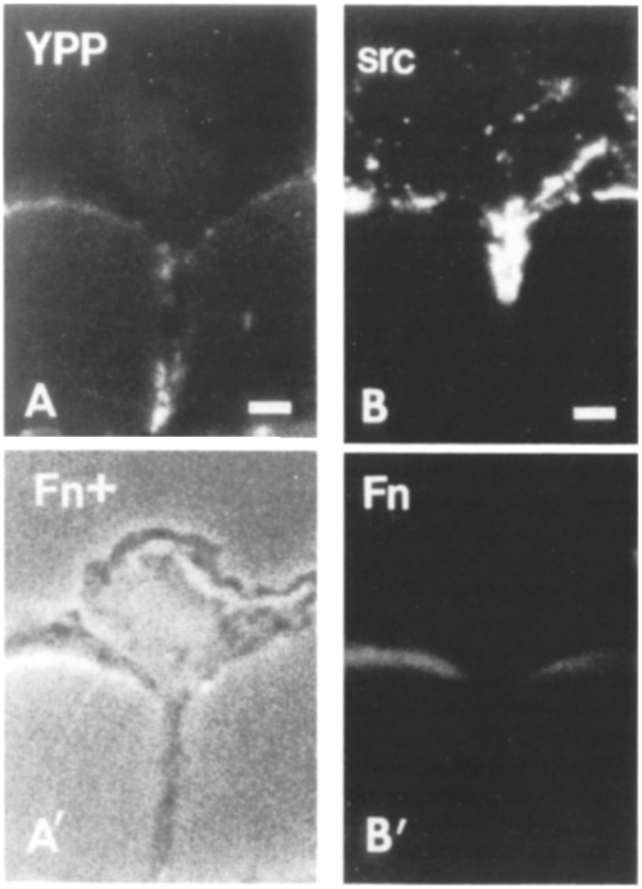

Figure 4. High magnification localization of YPP and pp60$^{v\text{-}src}$ in invadopodia. (*A*, *A'*): Cells were cultured on rhodamine–fibronectin beads, and indirectly labeled with mouse mAb 1G2 directed against YPPs, followed by a fluorescein conjugate of goat anti–mouse antibodies. YPPs are localized at the tip of a large invadopodium (*A*). In (*A'*), the micrograph is a composite of the phase-contrast image with the epifluorescence image of antifibronectin labeling (*Fn+*). (*B*, *B'*) Localized distribution of fibronectin (*Fn*) and pp60$^{v\text{-}src}$ (*src*) using double-label immunofluorescence microscopy. Sections were indirectly labeled with mouse mAb EB7 directed against an epitope of pp60$^{v\text{-}src}$, followed by rhodamine-conjugated goat anti–mouse IgG antibody and fluorescein-conjugated goat anti–chicken cellular fibronectin. The pp60$^{v\text{-}src}$ protein is localized at a large invadopodium extending into the bead where cells have locally degraded the labeled fibronectin surface (*B*, *B'*). Bar, 2.5 μm.

formation. The results of this experiment are found in Fig. 6. At 5 μg/ml genistein, YPP labeling of adhesion plaques was unaffected and the mobility of ruffling membranes on the dorsal surface where there was no apparent YPP labeling remained active. As the concentration of genistein was increased from 5–50 μg/ml, the cellular mobility was reduced progressively. At the low concentration (5 μg/ml) of genistein, the membrane localization of YPPs at invadopodia was reduced, although the intracellular or diffuse labeling still appeared relatively bright (Fig. 6, *36°C + Gt*). Thus, whereas labeling of YPPs at adhesion plaques appeared insensitive to the low concentrations of genistein used, the membrane localization of YPPs at invadopodia and fluorescent fibronectin removal were reduced by the genistein treatment.

*Table I. Frequency of Cells with Fibronectin Degradation and Invadopodia, pp60$^{v\text{-}src}$, and YPP in a Population of Normal or RSV-Transformed Cells**

Cell associated characteristic	Percent of transformed	Percent of normal
Degradation‡	48(5)§	0
Invadopodia‖	38(3)	0
pp60$^{v\text{-}src}$¶	81(7)	0
YPP**	56(4)	7(6)

* Cells were incubated with fibronectin–gelatin beads for 1 d and processed as described in Materials and Methods. The percent of cells that labeled with mAb CP1, a marker for invadopodia, anti-pp60$^{v\text{-}src}$, and anti-YPP was measured on 0.5-μm thin, frozen sections of cell–bead aggregates.

‡ Fibronectin degradation was visualized as localized sites of fluorescent fibronectin removal from the surface of the gelatin cross-linked substratum beneath cells.

§ For each experiment, numbers presented are percent of total cells counted and are given as the mean with the SD given in parentheses. Triplicate determinations were from independent cultures, and each determination was for 30 cells.

‖ Invadopodia were localized by indirect immunofluorescence microscopy using monoclonal CP1 antibody that co-localizes with sites of degradation at rosette contacts.

¶ Sections were indirectly labeled for immunofluorescence microscopy with mouse mAb EB7 directed against an epitope of viral pp60$^{v\text{-}src}$. In >40% of transformed cells, pp60$^{v\text{-}src}$ labeling was diffuse in the cytoplasm and neither extracellular proteolysis nor invadopodia was detected in these cells.

** YPPs in contact sites were visualized by indirect immunofluorescence using mouse mAb 1G2.

Image analysis was carried out to determine the relative amounts of YPP labeling in invadopodia versus adhesion plaques of individual transformed cells as shown in Figs. 5 *B* and 6 *B*. The data from three representative cells are shown in Fig. 7. In a noninvasive transformed cell, adhesion plaque labeling represents 100% of total ventral cell-surface labeling for YPP. In two invasive cells, invadopodia represents 81% and 45%, respectively, of total ventral cell-surface YPP labeling. The two invasive cells in these examples each have approximately sevenfold higher ventral YPP labeling than the noninvasive cell. This example serves to illustrate that invadopodial YPPs would be a significant component of the YPPs isolated from transformed cell contacts.

Identification of YPPs in Invadopodia

Considering the increased expression of YPPs in cells containing invadopodia and the fact that 56% of transformed cells contain invadopodia, we sought to isolate invadopodia from transformed cells and adhesion plaques from normal cells to compare their YPP composition on immunoblots using anti-YPP antibody. The identification of differences in the composition of YPPs associated with these structures might indicate those molecules that are involved in the function of invadopodia and uniquely associated with them. Cells were cultured on fibronectin, cross-linked gelatin films in tissue culture dishes, and the tenacity of cells adhering to gelatin films made it possible to shear away cell bodies, leaving behind invasive and noninvasive cell contacts.

Subconfluent layers of CEF or RSVCEF grown on gelatin films were sheared in the presence of 10 mM MOPS, pH 6.8, 100 mM KCl, 2.5 mM $MgCl_2$, 1 mM $CaCl_2$, 0.3 M sucrose, 1 mM Na_3VO_4, 0.02% NaN_3 at 4°C as described in the Materials and Methods. Immunofluorescent microscopy of membranes after shearing in shown in Figs. 8 and 9 *B* and *C*. In the case of contact membrane fragments from normal

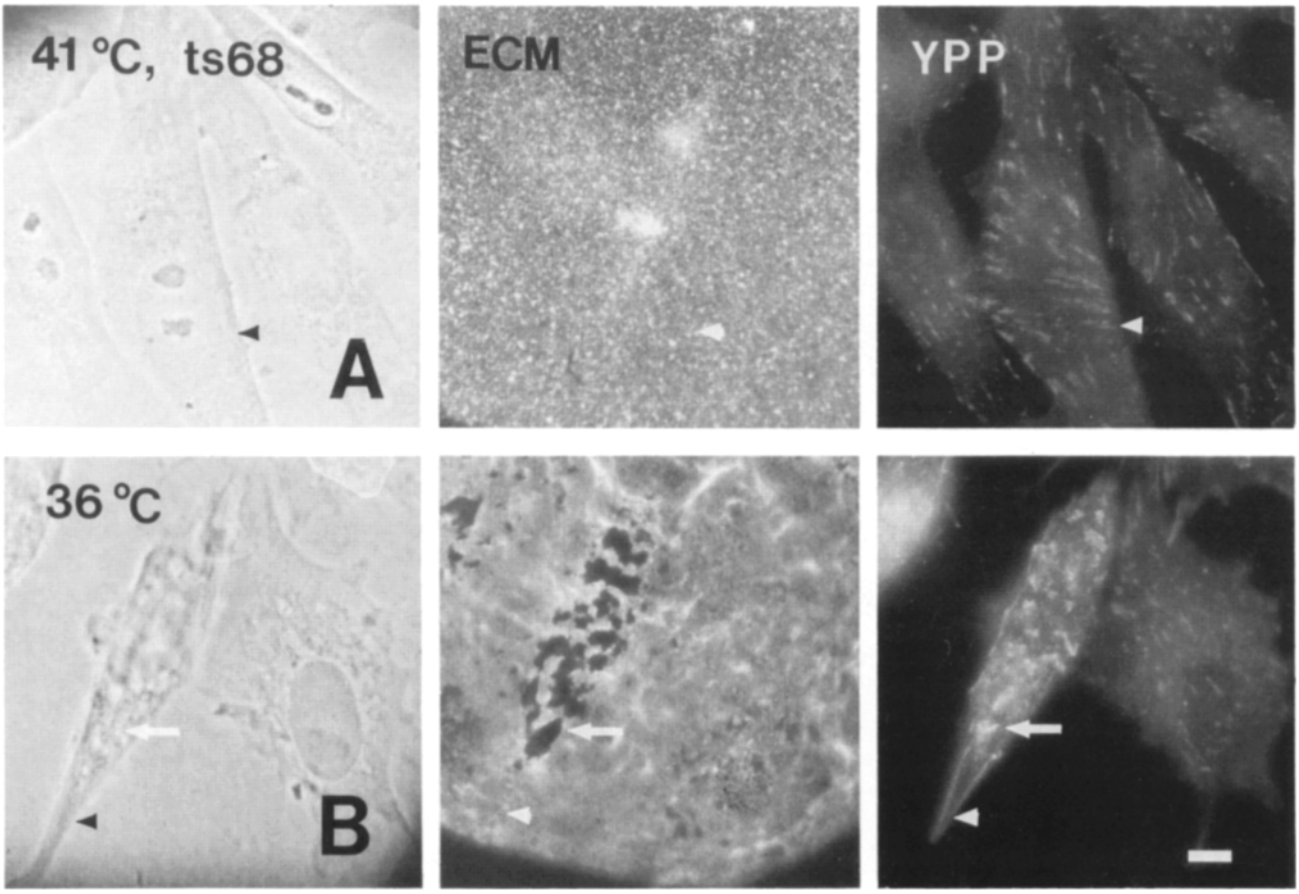

Figure 5. Low levels of YPPs are present in adhesion plaques of normal and transformed cells, but high levels are present in invadopodia. Whole cells grown on rhodamine–fibronectin-coated, thick, cross-linked gelatin films were fixed and permeabilized with Triton X-100. ts68 mutant RSV-infected CEF grown overnight at the nonpermissive temperature (row *A*) or the permissive temperature for cell transformation (row *B*) were photographed using phase-contrast microscopy (*left*). The fluorescent fibronectin-coated gelatin substratum was visualized using direct epifluorescence microscopy (*ECM*), and YPPs were visualized using indirect immunofluorescence microscopy of anti-YPP mAb staining (*YPP*). Cells at the nonpermissive temperature or permissive temperature contained YPP labeling of adhesion plaques (*arrowheads* in *A*, and cell at right in *B*, *YPP*), whereas transformed cells had bright labeling of invadopodia membranes associated with sites of fibronectin degradation (*arrows* in *B*, *ECM*, and *YPP*). Note lower level of YPP labeling at adhesion sites in a transformed cell (*arrowhead*, *B*). Bar, 10 μm.

cells, adhesion plaques that label for β_1 integrin are almost exclusively left behind after shearing, but actin filaments and the remainder of the ventral membrane have been removed (Fig. 8, *A–C*). In transformed cells, however, β_1 integrin-containing membrane sheets remained adherent to the gelatin surface, and showed a punctate actin distribution (Fig. 8 *E*) which was associated with a mottled Nomarski differential, interference-contrast pattern (Fig. 8 *F*) and with invadopodia which could be separately recognized by CP1 monoclonal antibody (Fig. 9, *B* and *C*). Immunoelectron microscopy of 0.1-μm thin, frozen sections reveals the morphology of invadopodia which are labeled for β_1 integrin (10 nm gold) and CP1 (5 nm gold) (Fig. 9 *A* and *inset*), and which correspond to the mottled Nomarski differential, interference-contrast pattern (Fig. 9, *B* and *C*). Thus, the punctate actin labeling (Fig. 8, *D–F*) likely represents actin-containing invadopodia where the cell body was sheared away.

After shearing away of cell bodies, the contact membranes and the gelatin matrix were vigorously scraped from the surface of the plastic dish using a cell scraper. This material was extracted with Triton X-114 into soluble and insoluble fractions, and the Triton X-114–soluble fraction was partitioned into aqueous and detergent phases. An amount from each fraction representing an equivalent amount of the crude extract was compared for transformed cell contacts by immunoblotting with mouse monoclonal anti-YPP antibody. Figure 10 illustrates that the majority of YPPs can be extracted from contact membranes in Triton X-114 and that they are mostly hydrophilic; they partition to the aqueous phase. Normal and transformed cell contacts were then compared on the same immunoblot (Fig. 11). Fig. 11, *A* and *B* are identical except that in *B*, 2 mM *O*-phospho-L-tyrosine was included in the incubation with anti-YPP mAb to demonstrate the specificity of the labeling patterns observed in *A*. Comparing 20 μl of normal cell contacts (Fig. 11, lane *N 20*) with 2 or 20 μl of transformed cell contacts (Fig. 11, lanes *T 20* and *T 2*) reveals a marked increase in YPPs from transformed cell contacts compared with normal contacts. Figure 11 *C* illustrates differences between normal (100 μl) and

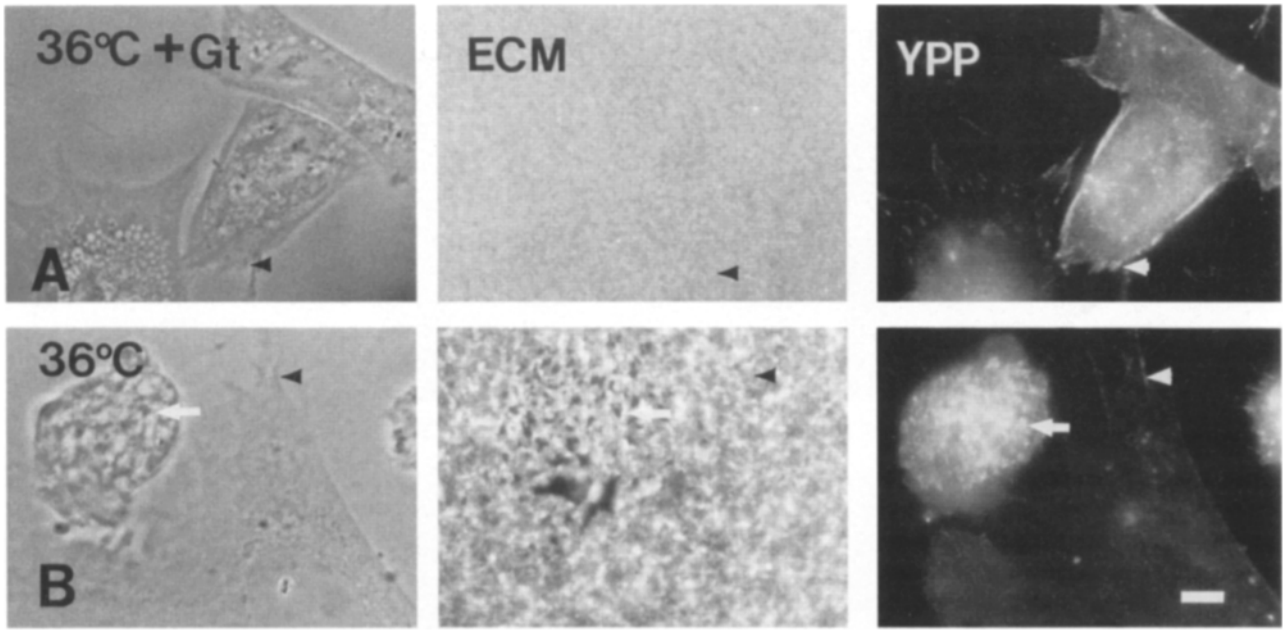

Figure 6. Inhibition of fluorescent fibronectin removal and membrane localization of YPP in invadopodia by genistein. Cells were cultured as described in Fig. 5. ts68 mutant RSV-infected cells were cultured for 4 h at the nonpermissive temperature and then shifted to the permissive temperature, 36°C, overnight in the presence or absence of genistein. Cells were photographed using phase-contrast microscopy (*left*). In row *A*, cells were treated with 5 μg/ml genistein (see Materials and Methods), and in row *B* the cells were treated with the solvent dimethyl sulfoxide in the absence of genistein. The fluorescent fibronectin-coated gelatin substratum was visualized using direct epifluorescence microscopy (*ECM*), and YPPs were visualized using indirect immunofluorescence microscopy of anti-YPP mAb staining (*YPP*). Cells, following treatment with genistein, did not remove the fluorescently labeled substratum, and YPP labeling of invadopodia at the membrane was reduced, although bright diffuse YPP labeling remained. Adhesion plaque staining in streaks was still apparent at the membrane (*arrowheads* in *A*, *ECM*, and *YPP*). In the absence of genistein, cells degraded the matrix and invadopodia were labeled with anti-YPP (*arrow* in *B*, *YPP*). No degradation was associated with adhesion plaques either in the presence or absence of genistein (*arrowheads* in *A* and *B*, *ECM*). Bar, 10 μm.

transformed (20 μl) cell contacts when more protein was run in the normal cell contact lane and the film exposure for transformed cell YPP was reduced. The major YPPs of normal contacts run as a smear at ~120–130 kD and at 71 kD

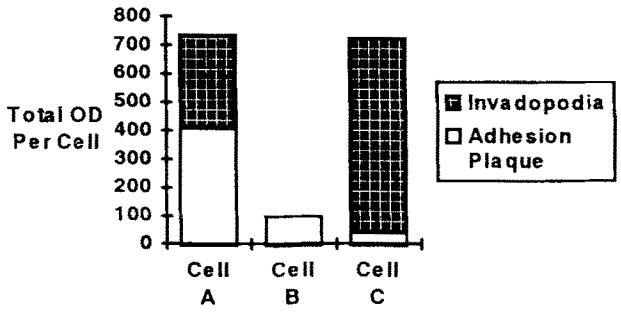

Figure 7. Distribution of YPP labeling in contacts of invasive and noninvasive cells. The total amount of YPP labeling attributable to invasive (*cells A* and *C*) versus noninvasive (*cell B*) contacts within a given cell was determined from a light micrograph negative containing YPP labeling of three representative transformed cells. The image was digitized using an image analysis system as described in the Materials and Methods. By summing the OD over the entire surface (pixels) of each contact and adding those amounts for all the contacts of a given type in that cell, invadopodia or adhesion plaques, a relative measure of total OD per cell and total OD for each contact type per cell was obtained which is comparable for the three cells.

in lanes where protein is somewhat overloaded (Fig. 11 *C*, *N 100*). At lower protein loadings, bands at 130 and 71 kD (Fig. 11 *A*, *N 20*) are detected. Transformed cell contacts have four major YPPs, at 150, 130, 81, and 77 kD. YPPs at 150, 81, and 77 kD appear to be absent in normal contacts, whereas YPP130 may be present in both normal and transformed cell contacts.

Tyrosine Phosphorylation of Membrane-Associated Proteins in Invadopodia

Paxillin and tensin, two cytoskeletal, tyrosine-phosphorylated proteins that are localized in adhesion plaques, were immunolabeled in whole, detergent-extracted cells cultured on fibronectin–gelatin cross-linked matrix. Tensin (Fig. 12, *A* and *B*) and paxillin (Fig. 12, *C* and *E*) labeling was found in patterns similar to those observed for YPPs at sites of localized degradation by transformed cells (some examples are indicated by *arrows*). Paxillin and tensin staining could be seen variously at invadopodia in rings at the center of cells (Fig. 12 *A–E*, for example). Paxillin staining was detectable in all cells and its absence in Fig. 12 *D* indicates the absence of a cell, as confirmed by Nomarski differential, interference-contrast microscopy (not shown). Thus, paxillin and tensin are two additional cytoskeletal proteins that together with a growing list of YPPs (25) would be isolated with adhesion plaque as well as invadopodial fractions.

To compare the specific enrichment of YPPs and known

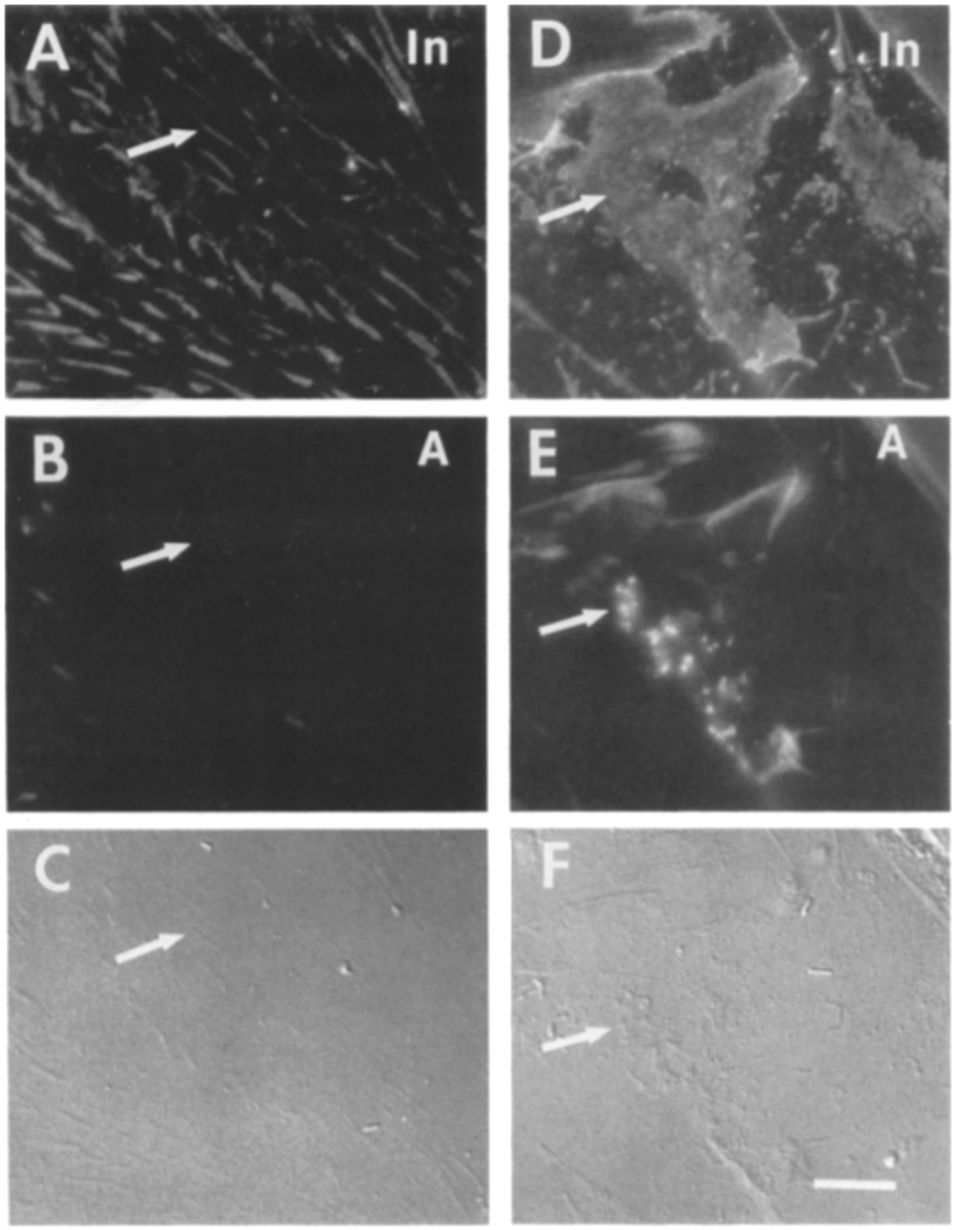

Figure 8. Actin and integrin are retained in isolated invadopodial membranes. Normal (*A–C*) and transformed cells (*D–F*) were cultured on cross-linked gelatin substratum overnight, cell bodies were sheared away, and then cells were fixed and stained with rat mAb ES238 followed by fluorescein-conjugated goat anti-rat antibody and rhodamine-phalloidin as described in Materials and Methods. Immunofluorescence microscoy of anti-β_1 integrin labeling (*In*) is shown in the top two panels (*A*, and *D*), and the rhodamine epifluorescence images of phalloidin labeling are shown in the middle panels (*B*, and *E*) revealing the distribution of actin (*A*). The bottom panels (*C*, and *F*) are the Nomarski differential interference-contrast images of the cellular material adhering to the surface of the gelatin cross-linked film. In normal cells, the majority of the cell body was sheared away from well-spread cells leaving behind membrane fragments at cell contact sites that were labeled by anti-integrin β_1 antibody (*arrow*, *A*) but only minimally by phalloidin (*arrow*, *B*). In contrast, profiles of ventral membranes of transformed cells showed diffuse integrin distribution (*D*), and actin localization in a rosette pattern (*arrow*, *E*) which coincides with the mottled Nomarski differential interference-contrast image. Bar, 10 μm.

cytoskeletal and membrane proteins in the invadopodia fraction, three subcellular fractions were prepared from cells cultured on the fibronectin–gelatin cross-linked matrix: supernate, cell body, and cell contact fractions (see Materials and Methods). These fractions from normal and transformed cells were first characterized with respect to the total protein recovered from each fraction and the percent total protein in each fraction (Table II). The differences in the distribution of protein between the supernate and cell body fractions and between normal and transformed cells is probably due to the fact that transformed cells are rounded, whereas the normal cells are well spread. The normal cells may fragment more after shearing, thus releasing an increased amount of soluble cytosolic proteins into the supernate.

Equal protein loadings (22 μg) of each fraction were compared after SDS-PAGE and immunoblotting using mouse monoclonal antiphosphotyrosine antibodies and antibodies against β_1 integrin, α-actinin, talin, vinculin, tensin, and paxillin (Fig. 13). Specific labeling of YPPs and these membrane-associated polypeptides in the subcellular fractions was estimated by densitometry and the ratios between the supernate or cell contact fraction and cell body obtained (Table II). Immunoblotting using mAb ES238 recognizing β_1 integrin was performed to follow the distribution of the plasma membrane since immunofluorescence microscopy demonstrates its localization at the plasma membrane of cells cultured on fibronectin–gelatin cross-linked matrices (34). Integrin β_1 present in the transformed cell supernate fraction (Fig. 13) may represent soluble proteins or alternatively, proteins associated with nonpelleting membrane vesicles. Talin, vinculin, and α-actinin are not enriched in the contact fractions or supernates relative to the cell bodies, however, tensin and paxillin are concentrated in the cell contact fraction and supernate, and are less prominent in the cell

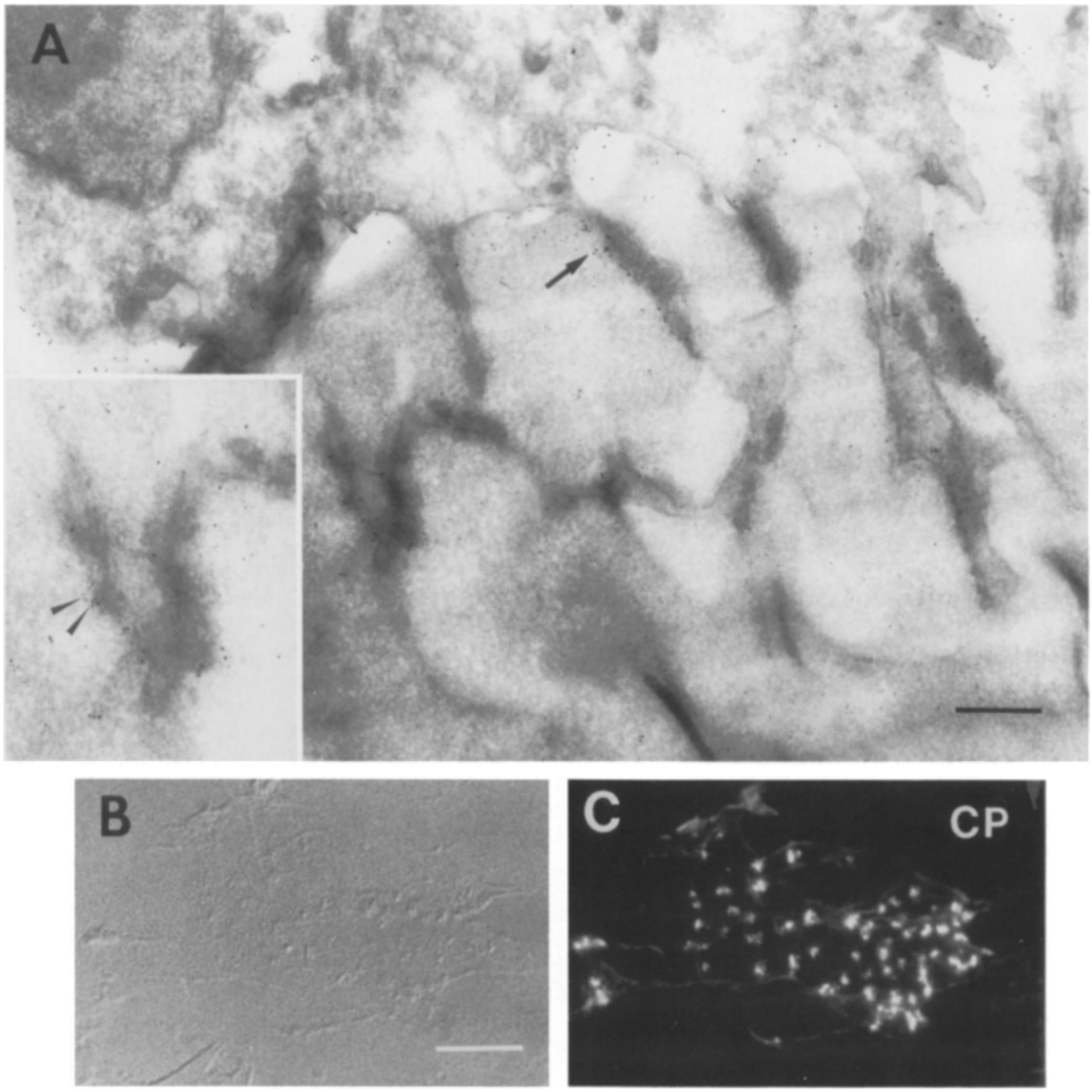

Figure 9. Invadopodia are labeled by the marker mAb CP1. (*A*) A transformed cell, cultured overnight on a cross-linked gelatin bead, has extensively invaded the bead as seen in this 0.1-μm thin, frozen section. Antiintegrin labeling (10 nm gold) is found over the membranes of some invadopodia (*arrow*). A 3× enlargement of an area immediately to the right of the inset shows the labeling of the invadopodial marker CP1 mAb (5 nm gold) which can be found over and near the membranes of invadopodia. Frozen sections were double immunolabeled with polyclonal rabbit anti-140K integrin complex antibody and rat monoclonal CP1, followed by 10 nm gold-conjugated anti-rabbit and 5 nm gold-conjugated anti-rat secondary antibodies. (*B* and *C*) Sheared ventral membranes from RSVCEF cultured overnight on cross-linked gelatin films were prepared for immunolabeling as described in Fig. 8. The films were immunolabeled with CP1, followed by fluorescein-conjugated goat anti-rat antibody. Immunofluorescence microscopy of the fluorescein image of CP1 labeling (*C*, *CP*) shows bright labeling of the welts seen by Nomarski differential interference-contrast microscopy (*B*). Bars, (*A*) 50 μm; (*B* and *C*) 20 μm.

body fraction (Fig. 13). In contrast to cytoskeletal proteins, the specific activity of the total YPPs isolated from RSVCEF contacts was ~38-fold higher than that of YPPs from CEF contacts (<1 versus 38, Table II; Fig. 13 *bottom panel*). YPPs were also enriched in the transformed cell contact fraction ~1.7 times more than YPPs from the transformed cell body fraction (Table II; Fig. 13 *bottom panel*). Comparison of the specific activities of YPP81/77 and YPP150 in cell contacts, cell bodies, and supernates, however, reveals a modest enrichment of the YPP81/77 in the cell contact fraction which paralleled the behavior of total YPPs (1.5- versus 1.7-fold enrichment over cell body), but a marked enrichment of the YPP150 in the cell contact fraction (3.6-fold over cell body) and also a twofold enrichment in the supernate fraction (Table II). Thus, the subcellular distribution of the tyrosine-phosphorylated YPP150 is similar to the distribution

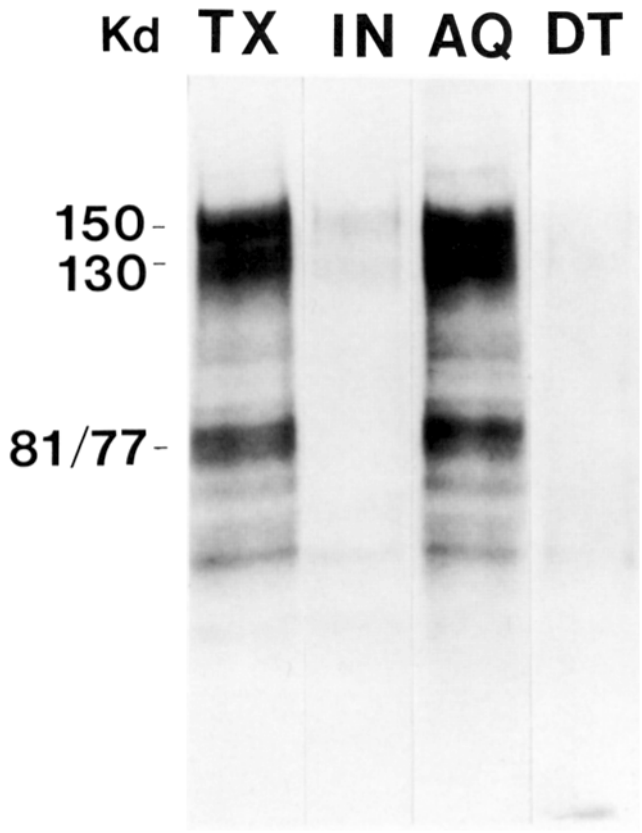

Figure 10. YPPs from transformed cell contacts are mostly Triton X-114–extractable and partition to the aqueous phase. Cell contacts were prepared from transformed cells cultured overnight on gelatin films in the presence of vanadate and extracted with Triton X-114 as described in Materials and Methods. The Triton X-114–soluble material (*TX*), the Triton X-114–insoluble material (*IN*), and the aqueous (*AQ*), and detergent phases (*DT*) were separated by SDS-PAGE and immunoblotted with mouse mAb 4G10 to identify the YPPs. Each lane represents an aliquot representing an equal volume from the original extract. Most of the YPPs are Triton X-114 soluble (*TX*) and partition to the aqueous phase (*AQ*). Molecular masses (kD) are given at left.

of tensin and paxillin, although the subcellular distribution of the unphosphorylated form of the YPP150 is unknown. Taken together, the fractionation and immunolocalization data are consistent with the interpretation that tyrosine-phosphorylated YPP150 is localized in invadopodia.

Discussion

Invadopodia, visualized using immunofluorescent and immunoelectron microscopy, are membrane protrusions which extend beneath the cell into the substratum after degradation of the exogenous fibronectin and gelatin matrix. They may also be involved in the internalization of digested matrix material (34). By using immunomicroscopy, we demonstrate that YPPs are localized in adhesion plaques from noninvading normal or transformed cells, but find that they are highly elevated in association with invadopodia, another class of contact, which are involved in substrate degradation and invasion. These results are consistent with previous morphological studies (31,37), and extend these observations to include the elevated expression of YPPs in invasive subcellular protrusions, invadopodia. It is suggested that tyrosine phosphorylations may regulate the invasive process mediated by invadopodia.

We have shown previously that within 10 min after contact of RSVCEF and beads, integrin and talin redistribute to sites of fibronectin–bead contact (36). YPP labeling can also be observed in patches at the fibronectin–bead contact sites (data not shown). As early as 1 h following contact, sites of fibronectin removal can be detected at which YPP labeling of membrane protrusions is prominent (Fig. 3). The events leading up to the formation of invasive structures within cells are thus rapid, occurring in <1 h, and the relevant YPPs, which may be involved in the formation of invadopodia are quickly accumulated at the plasma membrane, possibly within 10 min of contact with the substratum.

A morphological evaluation of invasive cells by visualization of degradation spots often allows a glimpse of the recent history of cells that are associated with the degradation spots since fluorescent fibronectin removal is a time-dependent, cumulative process. In contrast, localization of YPP, tensin, and paxillin appears to offer information on the location of the invasive lamellipodia of the cell, i.e., the currently active sites of invasion and degradation. The evidence for this is the coincidence of degradation spots with labeling for these antigens. However, YPP labeling and sites of fluorescent fibronectin removal are not perfectly coincident. As the cell migrates, but continues to invade into the substratum, the sites at which active degradation takes place change. YPP labeling may indicate putative sites of invasion, such as the formation of invasive protrusions just prior to the visual detection of fluorescent fibronectin removal.

By means of a novel cell fractionation procedure, we have isolated cell contacts from normal cells (adhesion plaques) and from transformed cell cultures (adhesion plaques plus invadopodia). The identity of the isolated contact sites adhering to the gelatin was determined by immunofluorescence microscopy using mAb CP1 recognizing invadopodia and anti-β_1 integrin antibody that labels the membrane fragments associated with invadopodia and adhesion plaques. Data on the YPP profiles of the isolated cell contacts, together with the results on the immunolocalization of YPPs in cells cultured on gelatin cross-linked matrix lead us to conclude that the YPP130 and YPP71 observed in immunoblots of CEF contacts represent the major membrane-associated YPPs present in adhesion plaques. We have achieved this without prior treatment of cells with vanadate or other reagents to enhance the recovery of the minor component of YPPs since we selectively enriched for membrane contact sites using cell fractionation. The increased amounts of YPPs in RSVCEF contacts compared to CEF contacts is consistent with the 10-fold overall increase in YPPs which was previously observed in whole cell extracts after transformation (24). We found that the specific activity of YPPs determined from immunoblots was estimated to be ~38-fold higher in cell contacts isolated from transformed cell contacts relative to contacts from untransformed cells. Image analysis of YPP immunolabeling of contacts within a transformed cell population demonstrates that contact YPP labeling from cells containing invadopodia may be as much as sevenfold higher than amounts localized in cells containing only adhesion plaques. Image analysis also resulted in an es-

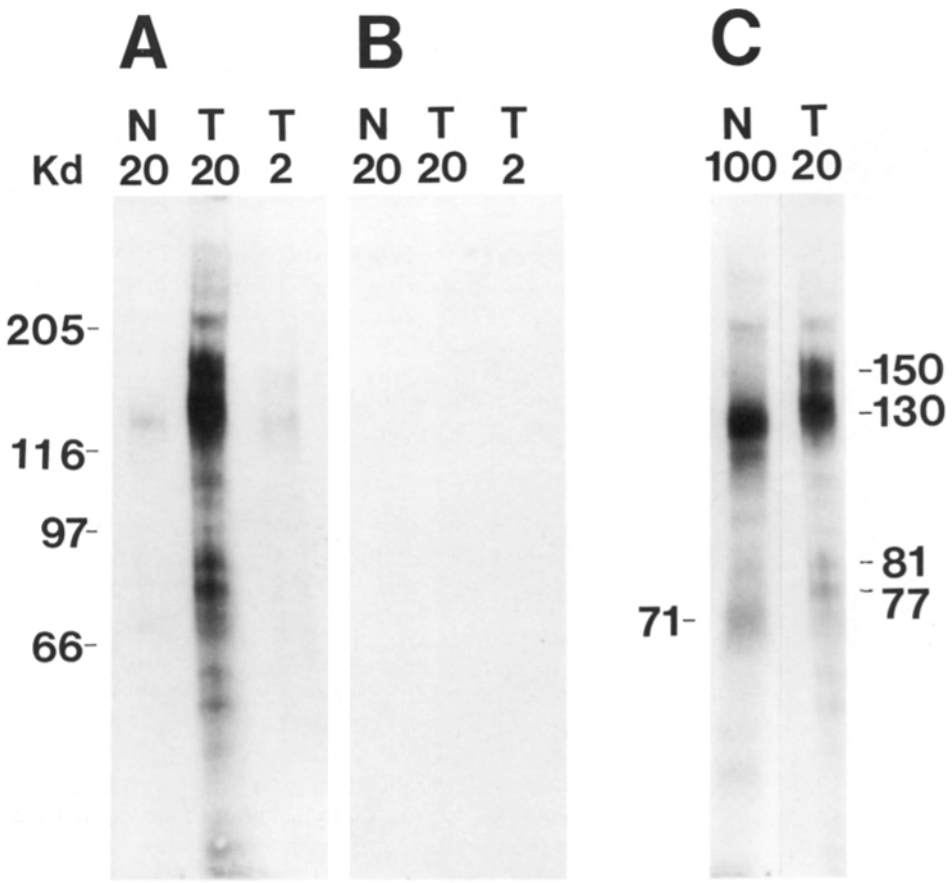

Figure 11. Identification of YPPs from transformed cell contact membranes that are absent from adhesion plaques of untransformed cells. Cell contacts from normal (*N*) or transformed (*T*) cells grown overnight on gelatin films were isolated in the presence of a vanadate-containing buffer as described in Materials and Methods. 20 μl of the total Triton X-114–soluble fraction from normal (lane *N 20*) and transformed (*T 20*) cells were compared, as well as 2 μl of RSVCEF contact membranes (*T 2*) (*A*). All samples were reduced and boiled. Immunoblots were probed using mouse mAb 4G10 in the absence (*A*) or presence of 2 mM *O*-phospho-L-tyrosine (*B*), followed by secondary goat anti-mouse conjugated to horseradish peroxidase. In (*C*), a lane containing 100 μl of ethanol precipitated contacts from untransformed cells (*N 100*) is shown. Lanes *N 100* and *T 20* were cut from the photograph of the gel and compared side-by-side. A smear of protein is seen at ~120–130 kD in the *N 100* and another band at 71 kD. In the transformed cell contacts, lane *T 20*, four major bands are observed, at 150, 130, 81, and 77 kD. Molecular masses (kD) are shown.

timation that more than 41% of the YPPs are contained in invadopodia and would thus significantly contribute to the YPP profile from isolated transformed cell contacts.

Comparison of cells cultured on plastic with cell bodies and cell contacts from cells cultured on matrix in the last three lanes of Fig. 13 demonstrates that cell contacts adhering to the matrix contain the highest specific activity of YPPs (Table II). To test whether genistein treatment grossly alters the specific activity of YPPs contained in isolated invadopodia, transformed cells were cultured overnight in the presence or absence of 5 μg/ml genistein after a period of 1 h for cell attachment. However, changes in the pattern of YPPs in subcellular fractions were not detectable on immunoblots (data not shown).

Differences in immunoblotting patterns were observed for talin, tensin, and paxillin that may reflect differences in the proteolytic milieu between cell body and cell contact fractions of normal and transformed cells or differences in secondary modifications of polypeptides. Comparison of talin between cell body and cell contact fractions, for example, reveals changes in the stoichiometry of the upper and lower immunoreactive bands of talin (Fig. 13, *talin*). The lower band likely represents a proteolytic fragment of talin, but it is not known if these differences arise before or after subcellular fractionation. Likewise, the multiple bands observed in the tensin blot may be due to the proteolytic sensitivity of the protein. With respect to paxillin, transformed cell fractions contain additional immunoreactive bands compared to fractions from normal cells. In addition, the profile of cell bodies and cell contacts is different. The significance of this is unknown, but these alterations may reflect changes in secondary modifications of paxillin in transformed cells and/or proteolytic variations in cell bodies versus cell contacts.

Comparison of normal contacts with transformed contacts not only reveals quantitative differences, but also qualitative differences in the detectable YPPs. In particular, a YPP migrating at ~150 kD appears to be transformation specific, occurring only in invasive cell contact fractions. Its three- to fourfold enrichment in the cell contact fraction compared with the cell body fraction of transformed cells and its similarity to the distributions of paxillin and tensin, two cytoskeletal proteins that are localized at normal and invasive cell contacts, is consistent with the interpretation that the phosphorylated form of this polypeptide is uniquely associated with invasive contacts. Recently, mAbs have been prepared against the transformation-sensitive YPPs from chicken cells (17,22,26,47). A YPP150 has not been described to our knowledge. Another molecule with similar molecular mass, phospholipase C-γ, that is involved in signal transduction mechanisms associated with tyrosine phos-

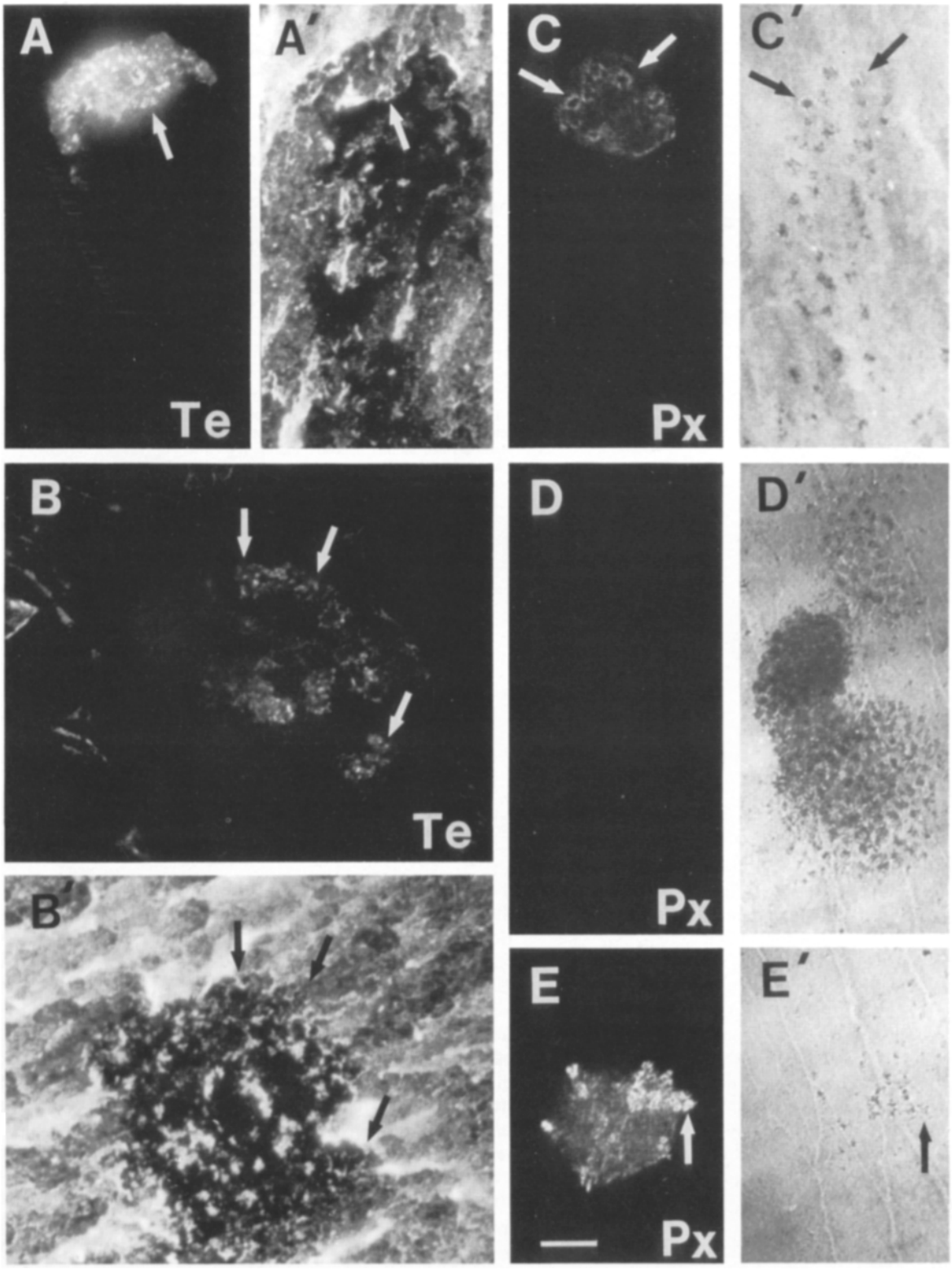

Figure 12. Paxillin and tensin localize in invadopodia at sites of matrix removal. (*A–E*) Cells were cultured on fluorescein-fibronectin beads, and indirectly labeled with mouse mAb antipaxillin or rabbit polyclonal antitensin as described in the Materials and Methods, followed by a rhodamine conjugate of goat anti-mouse or goat anti-rabbit antibodies, respectively. Tensin labeling of invadopodia in cells invading into the cross-linked substratum (*A* and *B*) co-localizes with sites of fluorescent fibronectin removal (*A'* and *B'*, *arrows*). Paxillin labeling of invadopodia (*C* and *E*) also co-localizes at sites of fluorescent fibronectin removal (*arrows*, *C'* and *E'*). Migrating invasive cells often leave behind "tracks" of fluorescent fibronectin removal (*A'*, *C'*, and *D'*), and occasionally the cell becomes detached at sites of extensive matrix removal (*D'*) as evidenced by the lack of cellular paxillin staining (*D*). The absence of a cell was confirmed by Nomarski differential, interference-contrast microscopy. Bar, 10 μm.

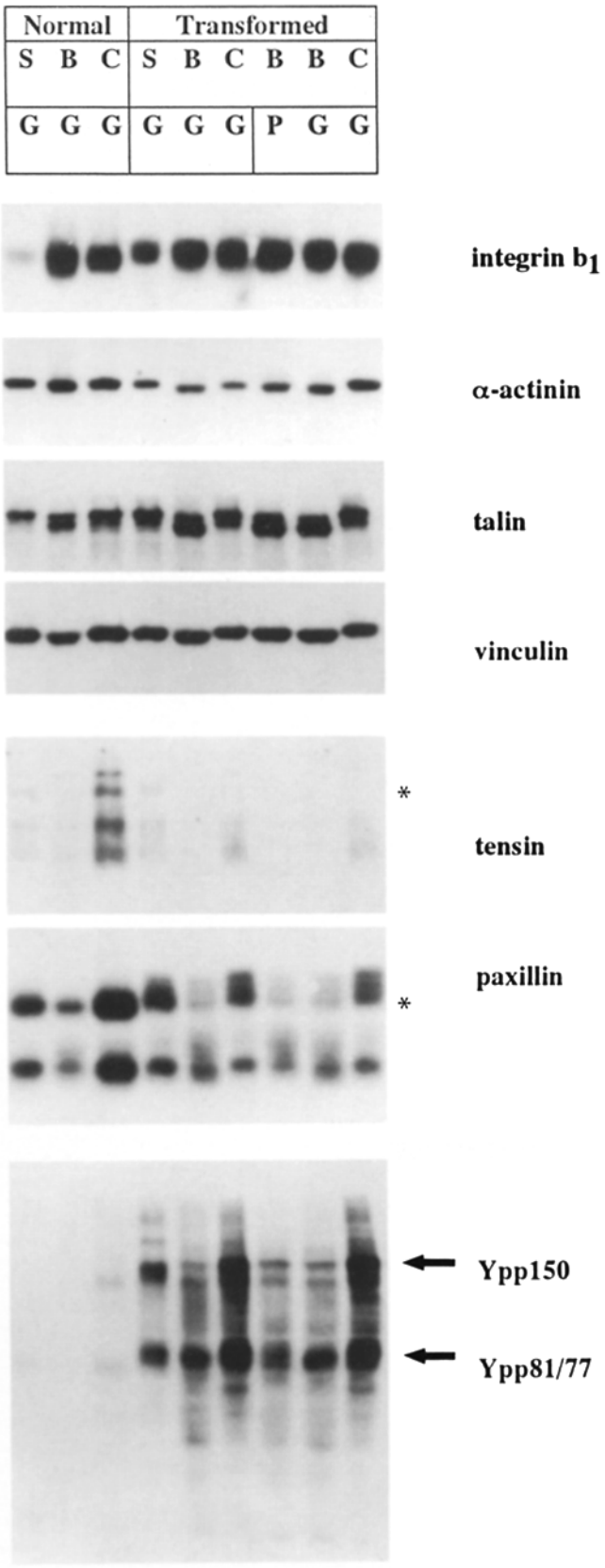

Figure 13. The distribution of YPPs, β_1 integrin, paxillin, tensin, talin, α-actinin, and vinculin in subcellular fractions from normal and transformed cells. Cell contacts from CEFs (*Normal*) or RSV-CEFs (*Transformed*) grown overnight on plastic tissue culture dishes (*P*) or gelatin films (*G*) were isolated in the presence of 10 mM MOPS, pH 6.8, 100 mM KCl, 2.5 mM $MgCl_2$, 1 mM $CaCl_2$, 0.3 M sucrose, and 1 mM Na_3VO_4, 0.2 mM PMSF by shearing away cell bodies as described in the Materials and Methods. The cell bodies were pelleted at top speed in a microfuge and a supernate (*S*) and cell body fraction were obtained. The contacts and cell bodies were extracted with Triton X-114 and the soluble fractions from the cell body (*B*) and contact membrane (*C*) were obtained. (*) highlights the major band for tensin and paxillin. 22 μg of protein was loaded in each lane. Immunoblotting of proteins was as described in the Materials and Methods.

*Table II. Distribution of Cell Contact-Associated Polypeptides within Subcellular Fractions: Determination of Specific Activities by Image Analysis of Immunoblots**

	Normal			Transformed		
	S‡	CB	C	S	CB	C
Total protein	0.98§ (52%)‖	0.69 (36%)	0.231 (12%)	0.86 (17%)	3.9 (76%)	0.37 (7%)
Integrin-β_1	5**(0.1)‡‡	73(1.0)	62(0.9)	33(0.5)	74(1.0)	66(0.9)
α-Actinin	44(0.8)	59(1.0)	62(1.1)	29(1.1)	27(1.0)	20(0.7)
Talin	98(0.8)	129(1.0)	156(1.2)	140(0.8)	187(1.0)	141(0.8)
Vinculin	76(1.5)	50(1.0)	91(1.8)	71(1.0)	69(1.0)	59(0.9)
Tensin	4(1.3)	3(1.0)	38(12.7)	3(-)	-§§	5(-)
Paxillin	40(2.2)	18(1.0)	83(4.6)	49(4.9)	10(1.0)	41(4.1)
YPP150	-(-)	-(-)	-(-)	48(2.0)	24(1.0)	87(3.6)
YPP81/77	-(-)	-(-)	-(-)	34(0.7)	48(1.0)	74(1.5)
Total YPP	-(-)	-(-)	-<1(-)	13(0.6)	22(1.0)	38(1.7)

* The densities of the first 6 lanes of each immunoblot shown in Fig. 13 were determined semiquantitatively using an image analyzer as described in the Materials and Methods section and the legend to Fig. 13.

‡ Methods: Contacts were isolated from normal (CEF) or transformed (RSVCEF) cells cultured on gelatin films by shearing away cell bodies as described in the Materials and Methods. The cell bodies were centrifuged and a supernate (*S*) and cell body fraction were obtained. The contact membranes adhering to the gelatin film were extracted with 1.3% Triton X-114 and the detergent soluble fractions from the cell body (*CB*) and contact membrane (*C*) fractions were obtained.

§ Mg of total Triton X-114–extractable protein in each fraction.

‖ The percent of the total Triton X-114–soluble protein contained within each fraction is given.

** Results are given in arbitrary units representing specific activities since each lane that was immunoblotted contained 22 μg protein. These specific activities are comparable for normal and transformed cell fractions for each polypeptide.

‡‡ Specific activities are given as a ratio relative to the specific activity in the cell body for normal or transformed cells.

§§ No detectable bands were observed or they were too low for densitometry.

phorylations, does not co-localize with sites of fluorescent fibronectin removal associated with invadopodia of transformed chicken cells (Mueller S. C., and W. -T. Chen, unpublished data).

Some of the major YPPs from transformed cell contacts may be related to those from normal contacts. For example, the p130 of transformed cells might be related to similarly migrating bands present in normal cell contacts. The YPP81/77 bands of transformed cells might be related to the YPP71 band from normal cell contacts, although the YPP81/77 bands consistently migrate more slowly than the band from normal cell contacts. YPPs are greatly enriched in transformed cell contacts compared to their specific activities in normal contacts. This increase may influence the adhesive and invasive properties of transformed cells. Future experiments will be directed towards determining the identity of the YPPs from transformed and normal cell contacts using existing and newly obtained mAb reagents against transformation-specific polypeptides, including testing the

possibility that the YPP71 band of normal cell contacts or YPP81/77 bands from transformed cells are related to paxillin, a recently described YPP (42), and that YPP130 may be related to previously described molecules with molecular masses of ~120 kD (19,26). Although the YPP150 comigrates with one of the major breakdown products of tensin and the YPP81/77 doublet comigrates with the two uppermost bands recognized by antipaxillin in transformed cell fractions, their identities are as yet unknown.

In conclusion, the ability to isolate invadopodia and adhesion plaques via a novel cell fractionation procedure has allowed identification of a YPP150, which is enriched in transformed cell contacts ~3.6-fold over its concentration in the cell body fraction. This polypeptide may represent an invadopodia-specific YPP that is functionally important during transformed cell invasion into the extracellular matrix. Future studies on the formation, function, and subcellular composition of these structures will be greatly facilitated using this combined biochemical and morphological approach to identify unique components of invadopodia.

We thank V. Papodapolous and T. Kelly for helpful discussions. We thank L.-B. Chen for the gift of antitensin antibody, K. Burridge for the gift of antitalin antibody, and T. Parsons for mutant RSV ts68.

This investigation was supported by Public Health Services grant R01 CA39077 and R01 HL-33711 to W. -T. Chen, and an American Heart Association grant-in-aid to S. C. Mueller.

Received for publication 1 January 1992 and in revised form 13 July 1992.

References

1. Akiyama, T., and H. Ogawara. 1991. Use and specificity of genistein as inhibitor of protein-tyrosine kinases. *Method Enzymol.* 201:362–370.
2. Akiyama, T., J. Ishida, S. Nakagawa, H. Ogawara, S. Watanabe, N. Itoh, M. Shibuya, and Y. Fukami. 1987. Genistein, a specific inhibitor of tyrosine-specific protein kinases. *J. Biol. Chem.* 262:5592–5595.
3. Aneskievich, B. J., B. Haimovich, and D. Boettiger. 1991. Phosphorylation of integrin in differentiating ts-Rous sarcoma virus-infected myogenic cells. *Oncogene.* 6:1381–1390.
4. Aoyama, A., and W. -T. Chen. 1990. A 170-kDa membrane-bound protease is associated with the expression of invasiveness by human malignant melanoma cells. *Proc. Natl. Acad. Sci. U.S.A.* 87:8296–8300.
5. Bishop, J. M. 1991. Molecular themes in oncogenesis. *Cell.* 64:235–248.
6. Bordier, C. 1981. Phase separation of integral membrane proteins in Triton X-114 solution. *J. Biol. Chem.* 256:1604–1607.
7. Bottaro, D. P., J. S. Rubin, D. L. Faletto, A. M. Chan, T. E. Kmiecik, G. F. Vande Woude, and S. A. Aaronson. 1991. Identification of the hepatocyte growth factor receptor as the c-met proto-oncogene product. *Science (Wash. DC).* 251:802–804.
8. Cantley, L. C., K. R. Auger, C. Carpenter, B. Duckworth, A. Graziani, R. Kapeller, and S. Soltoff. 1991. Oncogenes and signal transduction [published erratum appears in Cell 1991 May 31;65(5):following 914]. *Cell.* 64:281–302.
9. Chen, J. M., and W. -T. Chen. 1987. Fibronectin-degrading proteases from the membranes of transformed cells. *Cell.* 48:193–203.
10. Chen, W. -T. 1989. Proteolytic activity of specialized surface protrusions formed at rosette contact sites of transformed cells. *J. Exp. Zool.* 251:167–185.
11. Chen, W. -T., K. Olden, B. A. Bernard, and F. -F. Chu. 1984. Expression of transformation-associated protease(s) that degrade fibronectin at cell contact sites. *J. Cell Biol.* 98:1546–1555.
12. Chen, W. - T., J. M. Chen, S. J. Parsons, and J. T. Parsons. 1985. Local degradation of fibronectin at sites of expression of the transforming gene product pp60src. *Nature (Lond.).* 316:156–158.
13. David-Pfeuty, T., and S. J. Singer. 1980. Altered distributions of the cytoskeletal proteins vinculin and alpha-actinin in cultured fibroblasts transformed by Rous sarcoma virus. *Proc. Natl. Acad. Sci. U.S.A.* 77:6687–6691.
14. Davis, S., M. J. Lu, S. H. Lo, S. Lin, J. A. Butler, B. J. Drucker, T. M. Roberts, Q. An, and L. B. Chen. 1991. Presence of an SH2 domain in the actin-binding protein tensin. *Science (Wash. DC).* 252:712–718.
15. Fairbairn, S., R. Gilbert, G. Ojakian, R. Schwimmer, and J. P. Quigley. 1985. The extracellular matrix of normal chicken embryo fibroblasts: Its effect on transformed chicken fibroblasts and its proteolytic degradation by the transformants. *J. Cell Biol.* 101:1790–1798.
16. Gavrilovic, J., G. Moens, J. P. Thiery, and J. Jouanneaut. 1991. Expression of transfected transforming growth factor α induces a motile fibroblast-like phenotype with extracellular matrix-degrading potential in a rat bladder carcinoma cell line. *Cell Regul.* 1:1003–1014.
17. Glenney, J. R., Jr. and L. Zokas. 1989. Novel tyrosine kinase substrates from Rous sarcoma virus-transformed cells are present in the membrane skeleton. *J. Cell Biol.* 108:2401–2408.
18. Glenney, J. R., Jr., W. S. Chen, C. S. Lazar, G. M. Walton, L. M. Zokas, M. G. Rosenfeld, and G. N. Gill. 1991. Ligand-induced endocytosis of the EGF receptor is blocked by mutational inactivation and by microinjection of anti-phosphotyrosine antibodies. *Cell.* 52:675–684.
19. Guan, J. L., J. E. Trevithick, and R. O. Hynes. 1991. Fibronectin integrin interaction induces tyrosine phosphorylation of a 120-Kda protein. *Cell Regul.* 2:951–964.
20. Guirguis, R., I. Margulies, G. Taraboletti, E. Schiffmann, and L. Liotta. 1987. Cytokine-induced pseudopodial protrusion is coupled to tumour cell migration. *Nature (Lond.).* 329:261–263.
21. Haimovich, B., B. J. Aneskievich, and D. Boettiger. 1991. Cellular partitioning of Beta-1 integrins and their phosphorylated forms is altered after transformation by Rous sarcoma virus or treatment with cytochalasin D. *Cell Regul.* 2:271–283.
22. Hamaguchi, M., M. Matsuda, and H. Hanafusa. 1990. A glycoprotein in the plasma membrane matrix as a major potential substrate of p60v-src. *Mol. Cell Biol.* 10:830–836.
23. Horvath, A. R., M. A. Elmore, and S. Kellie. 1990. Differential tyrosine-specific phosphorylation of integrin in Rous sarcoma virus transformed cells with differing transformed phenotypes. *Oncogene.* 5:1349–1357.
24. Hunter, T., and B. M. Sefton. 1980. Transforming gene product of Rous sarcoma virus phosphorylates tyrosine. *Proc. Natl. Acad. Sci. U.S.A.* 77:1311–1315.
25. Hynes, R. O. 1992. Integrins: Versatility, modulation, and signaling in cell adhesion. *Cell.* 69:11–25.
26. Kanner, S. B., A. B. Reynolds, R. R. Vines, and J. T. Parsons. 1990. Monoclonal antibodies to individual tyrosine-phosphorylated protein substrates of oncogene-encoded tyrosine kinases. *Proc. Natl. Acad. Sci. U.S.A.* 87:3328–3332.
27. Kellie, S., A. R. Horvath, and M. A. Elmore. 1991. Cytoskeletal targets for oncogenic tyrosine kinases. *J. Cell Sci.* 99:207–211.
28. Koch, C. A., D. Anderson, M. F. Moran, C. Ellis, and T. Pawson. 1991. SH2 and SH3 Domains: Elements that control interactions of cytoplasmic signaling proteins. *Science (Wash. DC).* 252:668–674.
29. Kramer, R. H., K. G. Bensch, and J. Wong. 1986. Invasion of reconstituted basement membrane matrix by metastatic human tumor cells. *Cancer Res.* 46:1980–1989.
30. Laemmli, U. K. 1970. Cleavage of structural proteins during the assembly of the head of bacteriophage T4. *Nature (Lond.).* 227:680–685.
31. Maher, P. A., E. B. Pasquale, J. Y. Wang, and S. J. Singer. 1985. Phosphotyrosine-containing proteins are concentrated in focal adhesions and intercellular junctions in normal cells. *Proc. Natl. Acad. Sci. U.S.A.* 82:6576–6580.
32. Maness, P. F., C. G. Shores, and M. Ignelzi. 1990. Localization of the normal cellular src protein to the growth cone of differentiating neurons in brain and retina. *Adv. Exp. Med. Biol.* 265:117–125.
33. Markwell, M. A., S. M. Hass, C. C. Bieber, and N. E. Tolbert. 1978. A modification of the Lowry procedure to simplify protein determination in membrane and lipoprotein samples. *Anal. Biochem.* 87:206–210.
34. Mueller, S. C., and W.-T. Chen. 1991. Cellular invasion into matrix beads: localization of beta 1 integrins and fibronectin to the invadopodia. *J. Cell Sci.* 99:213–225.
35. Mueller, S. C., T. Hasegawa, S. S. Yamada, K. M. Yamada, and W.-T. Chen. 1988. Transmembrane orientation of the fibronectin receptor complex (integrin) demonstrated directly by a combination of immunocytochemical approaches. *J. Histochem. Cytochem.* 36:297–306.
36. Mueller, S. C., T. Kelly, M. Z. Dai, H. N. Dai, and W.-T. Chen. 1989. Dynamic cytoskeleton-integrin associations induced by cell binding to immobilized fibronectin. *J. Cell Biol.* 109:3455–3464.
37. Nermut, M. V., P. Eason, E. M. Hirst, and S. Kellie. 1991. Cell/substratum adhesions in RSV-transformed rat fibroblasts. *Exp. Cell Res.* 193:382–397.
38. Pienta, K. J., W. B. Isaacs, D. Vindivich, and D. S. Coffey. 1991. The effects of basic fibroblast growth factor and suramin on cell motility and growth of rat prostate cancer cells. *J. Urol.* 145:199–202.
39. Saling, P. M. 1991. How the egg regulates sperm function during gamete interaction: Facts and fantasies. *Biol. Reprod.* 44:246–251.
40. Tapley, P., A. Horwitz, C. Buck, K. Duggan, and L. Rohrschneider. 1989. Integrins isolated from Rous sarcoma virus-transformed chicken embryo fibroblasts. *Oncogene.* 4:325–333.
41. Tarone, G., D. Cirillo, F. G. Giancotti, P. M. Comoglio, and P. C. Marchisio. 1985. Rous sarcoma virus-transformed fibroblasts adhere primarily at discrete protrusions of the ventral membrane called podosomes. *Exp. Cell Res.* 159:141–157.
42. Turner, C. E., J. R. Glenney, Jr., and K. Burridge. 1990. Paxillin: a new vinculin-binding protein present in focal adhesions. *J. Cell Biol.* 111:1059–1068.

43. Ullrich, A., and J. Schlessinger. 1990. Signal transduction by receptors with tyrosine kinase activity. *Cell.* 61:203–212.
44. Weber, M. J., A. H. Hale, and L. Losasso. 1977. Decreased adherence to the substrate in Rous sarcoma virus-transformed chicken embryo fibroblasts. *Cell.* 10:45–51.
45. Werb, Z., P. M. Tremble, O. Behrendtsen, E. Crowley, and C. H. Damsky. 1989. Signal transduction through the fibronectin receptor induces collagenase and stromelysin gene expression. *J. Cell Biol.* 109:877–889.
46. Willingham, M. C., K. M. Yamada, S. S. Yamada, J. Pouyssegur, and I. Pastan. 1977. Microfilament bundles and cell shape are related to adhesiveness to substratum and are dissociable from growth control in cultured fibroblasts. *Cell.* 10:375–380.
47. Wu, H., A. B. Reynolds, S. B. Kanner, R. R. Vines, and J. T. Parsons. 1991. Identification and characterization of a novel cytoskeleton-associated pp60src substrate. *Mol. Cell Biol.* 11:5113–5124.
48. Yamada, K. M. 1978. Immunological characterization of a major transformation-sensitive fibroblast cell surface glycoprotein: localization, redistribution, and role in cell shape. *J. Cell Biol.* 78:520–541.